Published in final edited form as:

Circulation. 2015 March 24; 131(12): 1082–1097. doi:10.1161/CIRCULATIONAHA.114.012725.

Thioredoxin-2 Inhibits Mitochondrial ROS Generation and ASK1 Activity to Maintain Cardiac Function

Qunhua Huang, Ph.D[1,*], **Huanjiao Jenny Zhou, M.D, Ph.D**[1,2,*], **Haifeng Zhang, Ph.D**[1], **Yan Huang, Ph.D**[1], **Ford Hinojosa-Kirschenbaum, B.S**[3], **Peidong Fan, Ph.D**[3], **Lina Yao, Ph.D**[3], **Luiz Belardinelli, M.D**[3], **George Tellides, M.D., Ph.D**[4], **Frank J. Giordano, M.D**[1], **Grant R. Budas, Ph.D**[3], and **Wang Min, Ph.D**[1,2]

[1]Interdepartmental Program in Vascular Biology and Therapeutics, Department of Pathology, University School of Medicine, New Haven, CT

[2]Center for Translational Medicine, The First Affiliated Hospital, Sun Yat-Sen University, Guangzhou, China

[3]Gilead Sciences Inc., Foster City, CA

[4]Department of Surgery, Yale University School of Medicine, New Haven, CT

Abstract

Background—Thioredoxin 2 (Trx2) is a key mitochondrial protein which regulates cellular redox and survival by suppressing mitochondrial ROS generation and by inhibiting apoptosis stress kinase-1 (ASK1)-dependent apoptotic signaling. To date, the role of the mitochondrial Trx2 system in heart failure pathogenesis has not been investigated.

Methods and Results—Western blot and histological analysis revealed that Trx2 protein expression levels were reduced in hearts from patients with dilated cardiomyopathy (DCM), with a concomitant increase in increased ASK1 phosphorylation/activity. Cardiac-specific Trx2 knockout mice (Trx2-cKO). Trx2-cKO mice develop spontaneous DCM at 1 month of age with increased heart size, reduced ventricular wall thickness, and a progressive decline in left ventricular (LV) contractile function, resulting in mortality due to heart failure by ~4 months of age. The progressive decline in cardiac function observed in Trx2-cKO mice was accompanied by disruption of mitochondrial ultrastructure, mitochondrial membrane depolarization, increased mitochondrial ROS generation and reduced ATP production, correlating with increased ASK1 signaling and increased cardiomyocyte apoptosis. Chronic administration of a highly selective ASK1 inhibitor improved cardiac phenotype and reduced maladaptive LV remodeling with significant reductions in oxidative stress, apoptosis, fibrosis and cardiac failure. Cellular data from Trx2-deficient cardiomyocytes demonstrated that ASK1 inhibition reduced apoptosis and reduced mitochondrial ROS generation.

Correspondence: Wang Min, PhD, Interdepartmental Program in Vascular Biology and Therapeutics, Department of Pathology, Yale University School of Medicine, 10 Amistad St., New Haven, CT 06520, Phone: 203-785-6047, Fax: 203-737-2293, wang.min@yale.edu.

*contributed equally

Disclosures: None.

Conclusions—Our data support an essential role for mitochondrial Trx2 in preserving cardiac function by suppressing mitochondrial ROS production and ASK1-dependent apoptosis. Inhibition of ASK1 represents a promising therapeutic strategy for the treatment of dilated cardiomyopathy and heart failure.

Keywords

INTRODUCTION

Heart failure is a common clinical condition with a high morbidity and mortality[1, 2]. Conditions including dilated cardiomyopathy, inherited cardiomyopathy, diabetic cardiomyopathy, cardiac hypertrophy, and myocardial infarction, can all eventually result in heart failure. Results from human studies and animal models have suggested that the development of heart failure is associated with increased levels of reactive oxygen species (ROS)[3–6]. Apoptosis of cardiomyocytes, induced by ROS, has been causally linked to the pathogenesis of heart failure[7, 8]. However, the mechanisms by which ROS contribute to the development of heart failure remain unclear.

The thioredoxin (Trx) system, which involves thioreodoxin (Trx), Trx reductase (TrxR), and peroxidase (Prx), is an important regulator of cellular redox state[9–11]. Trxs are small redox proteins characterized by their proximate cysteines in a CXXC motif. Trx can reduce target proteins *via* cysteine thiol-disulfide exchanges. Trx-dependent Prx can also directly scavenge ROS (H_2O_2). In turn, TrxR converts oxidized Trx to its reduced form to facilitate its redox activity. Cytosolic Trx consists of Trx1, Trx1 reductase (TrxR1) and Trx1-dependent peroxidase. The mitochondrial-specific Trx system is comprised of Trx2, Trx2 reductase (TrxR2) and peroxiredoxin-3 (Prx3) andis highly expressed in tissues with high metabolic demand, such as the heart, brain, and liver[9–11]. In addition to their role in regulating cellular redox state, both cytosolic Trx1 and mitochondrial Trx2 are capable of forming a complex with apoptosis signal-regulating kinase 1 (ASK1), a redox-sensitive serine/threonine kinase that is activated in response to oxidative stress[12]. Upon an increase in cellular ROS, critical cysteine residues in Trx become oxidized, and Trx is dissociated from the Trx-ASK1 complex, resulting in auto-activation of ASK1 and induction of mitochondrial-dependent apoptotic cell death pathways[13, 14].

Global gene knockout of Trx1, TrxR1, Trx2 or TrxR2 causes embryonic lethality, which is likely due to increased cellular oxidative stress[15–18]. Trx1 knockout mouse embryos die shortly after implantation due to proliferation defects of the inner cell mass cells[19]. Mouse embryos with a global deletion of TrxR1 display severe growth retardation and have reduced cell proliferation similar to that observed in Trx1 deficient mice[18]. Although a global deletion of Trx2 or TrxR2 also causes early embryonic lethality, it appears that this effect is due to cellular apoptosis[15–17]. TrxR2 deficient embryos also exhibit severe anemia with defects in hematopoiesis, increased apoptosis in the liver, and thinning of the heart ventricular wall[15]. Heart-specific deletions of TrxR1 or TrxR2 have been reported. Mice with a heart-specific inactivation of TrxR1 develop normally and appear healthy[18]. In contrast, cardiac tissue-restricted ablation of TrxR2 results in fatal dilated cardiomyopathy, a

condition reminiscent of Keshan disease and Friedreich's ataxia[15, 18]. Indeed, a recent clinical genetic study identified loss-of-function mutations in TrxR2 in patients with dilated cardiomyopathy[20]. Based on these findings, it has been suggested that the mitochondrial Trx2/TrxR2 system is essential for normal cardiac function[15, 18].

Interestingly, mice with inducible cardiac-specific deletion of TrxR2 do not develop dilated cardiomyopathy, but these mice do exhibit exacerbated damage after ischemia/reperfusion injury. Because Trx2, (rather then TrxR2) directly catalyzes mitochondrial thiol-disulfide exchanges and ROS scavenging, we reasoned that the expression or/and activity of Trx2 is critical to maintain normal cardiac function. However, the role of Trx2 in heart development and pathogenesis has yet to be determined, as the Trx2 knockout is embryonically lethal.. Therefore, we examined Trx2 expression in human hearts with cardiomyopathy and investigated the intrinsic role of Trx2 in the heart by developing and characterizing mice with a cardiac-specific deletion of Trx2.

MATERIALS AND METHODS

Clinical specimens were collected from normal and diseased hearts during surgical procedures with approval from the relevant institutional review boards. All animal studies were approved by the Institutional Animal Care and Use Committee of Yale University. Expanded materials and methods are provided in the online supplement. These methods include human sample collection, generation of mice with a cardiomyocyte-specific deletion of Trx2 (Trx2-cKO), cell culture, immunoblotting and antibodies, immunogold electron microscopy, histology and immunohistochemistry, and mitochondrial DNA quantification, mitochondria isolation, Trx2 activity assay, measurements of mitochondrial mass, mitochondrial membrane potential ($\Delta\Psi m$) and ATP production as we described previously[21, 22]. Gene expression was performed using the NanoString nCounter system.

Generation of mice with a cardiomyocyte-specific deletion of Trx2 (Trx2-cKO)

The Trx2 targeting vector was constructed in a pEASYflox vector containing the 5' arm of homology (upstream of exon 3), knockout arm (exon 3) and 3' arm of homology (downstream of exon 3) of the Trx2 gene (see Supplemental data for details). Trx2 floxed-allele mice ($Trx2^{lox/lox}$), in which lox-P sites bracket exon 3, have no basal phenotype. $Trx2^{lox/lox}$ mice were backcrossed with C57BL/6 mice for more than six generations. $Trx2^{lox/lox}$ mice were crossed with α-myosin heavy chain (α-MHC)-Cre mice (C57BL/6 background) in which the Cre recombinase expression is driven by the α-MHC promoter to generate mice with cardiac myocyte-specific deletion of Trx2 ($Trx2^{lox/lox}$:MHC-Cre, designated Trx2-cKO). The MHC promoter is widely used to study gene function in cardiac pathogenesis[23]. This promoter is restricted to cardiac myocytes and is expressed only in the artria during embryonic development, and in both the atria and ventricles immediately before birth when it becomes a predominant isoform during adulthood[23]. Exon 3 of the Trx2 gene encodes a region containing the $WC^{90}GPC^{93}G$ functional motif which is deleted in hearts of the Trx2-cKO mice, leading to a frameshift of the downstream coding sequence, resulting in a complete loss of Trx2 expression specifically in cardiomyocytes. All experiments were performed with Trx2-cKO and $Trx2^{lox/lox}$ littermates were used as

controls. Mice were cared for in accordance with National Institutes of Health guidelines, and all procedures were approved by the Yale University Animal Care and Use Committee.

Administration of ASK1i in mice

ASK1i (GS-444217; 30 mg/kg) or vehicle control was administered once per day by oral gavage to littermate Ctrl or Trx2-cKO pups from P10 until P27. The mice were then administered ASK1i *ad libitum* in regular chow (0.2% GS-444217) starting from P30. Ctrl mice and vehicle groups were used as controls.

Hemodynamic and echocardiographic measurements

Anesthesia was induced by intraperitoneal injection of Ketamine (100mg/kg)/ Xylazine(10mg/kg). Mice were then intubated, placed on positive pressure ventilation and light anesthesia maintained by inhaled isofluorane. The right common jugular vein was cannulated with polyethylene tubing and a 1.9 French transducertipped catheter (Millar Inc., Houston, TX) was advanced into the left ventricular via the right carotid artery. Left ventricular pressures, including high-fidelity positive and negative dP/dt, were measured under basal conditions. Data were recorded by using MacLab software and were analyzed by using the Heartbeat program (UC San Diego; 19). Echocardiograms were obtained on lightly anesthetized mice (isofluorane inhalation via nosecone) by using the Vevo770 system (VisualSonics, Toronto, Canada) with a 40 MHz probe. Zoomed 2D images were used to determine a short axis plane at the level of the papillary muscles and then M-mode was obtained at this level. Measurements were obtained using the Vevo770 analysis software

Number of animals

Separate cohorts of animals were used for the different studies. The survival study observed 64 animals up to 140 days. Additionally, >200 mice were sacrificed at various times from 3 days to 3 months of age for diverse analytical procedures, many of which required different processing of the samples.

Data and Statistical Analysis

Data are represented as mean±SEM. Comparisons between two groups were by unpaired t-test, between more than two groups by one-way ANOVA followed by Bonferroni's post-hoc test or by two-way ANOVA, and between groups of results over time by repeated measures ANOVA. Analyses were performed using Prism 4.0 software (GraphPad). *P* values were two-tailed and values <0.05 were considered to indicate statistical significance. By considering the random effects for factors "heart" and "field" for ASK1 expressing cells of human heart tissues detected by immunohistochemistry, data were also analyzed by mixed effects model. For Mixed effect model calculation, the R Software for statistical computing, lme4 package (Linear mixed-effects models using Eigen and S4) and lmerTest package were used to calculate mixed-effects model.

RESULTS

Human hearts with dilated cardiomyopathy show reduced Trx2 expression and increased ASK1 activity

Since an association of Trx2 gene mutations with human dilated cardiomyopathy has not been found, we investigated whether Trx2 expression might be reduced in human hearts with cardiomyopathy. Hence, we measured Trx2 expression in myocardium from organ donors with preserved cardiac function (normal heart) and cardiac transplant recipients with severe idiopathic dilated cardiomyopathy (DCM) (Supplemental Fig.1). Trx2 expression was significantly reduced in idiopathic DCM (Fig.1A with quantification in 1B). Dimerization of Trx2-dependent peroxidase Prx3, an indicator of oxidative stress[24], was significantly increased in idiopathic DCM (Fig.1A with quantification in 1C). TrxR2 expression was increased, possibly as a compensatory mechanism for reduced Trx2 (Fig.1A with quantification in 1D). However, Trx1 levels were comparable between normal and idiopathic DCM groups (Fig.1A with quantification in 1E). Consistent with an inhibitory effect of Trx2 on ASK1 activity and apoptosis[14], the phosphorylation of ASK1 and active caspase-3 were significantly increased in idiopathic DCM (Fig.1A with quantification in 1F,G). The presence of severe coronary disease in an additional group of organ donors with preserved cardiac function did not significantly alter Trx2 expression or ASK1 activation in the myocardium (data not shown). We also determined the expression of Trx2 and ASK1 by histological analysis. Myocardium from patients with cardiomyopathy exhibited reduced Trx2 expression concomitant with increased ASK1 detection from few to around one-third of cardiomyocytes (Fig.1H), further suggesting the importance of Trx2 in maintaining normal myocardial function by inhibiting oxidative stress and ASK1.

Mice with cardiac-specific deletion (Trx2-cKO) develop dilated cardiomyopathy

Embryonic lethality due to global knockout of Trx2 in mice precludes a thorough analysis of the function of Trx2 in cardiac function in the post-developmental setting[15–18]. Therefore, we created cardiac-specific Trx2 knockout (Trx2-cKO) mice by breeding $Trx2^{lox/lox}$ with MHC-Cre mice in which Cre recombinase is driven by the cardiac-specific α-myosin heavy chain promoter (MHC-Cre) (Supplemental Fig.2A–B). A specific deletion of Trx2 in the Trx2-cKO heart was verified by the following approaches: 1) genotyping of genomic DNA with primers for the KO allele which was detected specifically in heart (Supplemental Fig. 2C), but not in other tissues; 2) immunostaining with anti-Trx2 antibody (which is a polyclonal generated with the Trx2 full-length protein as an antigen and recognizes all truncated Trx2 if any) in heart tissue detected Trx2 in vascular endothelium but not in the cardiomyocytes (Supplemental Fig.2D); 3) immunoblotting with anti-Trx2 antibody detected Trx2 protein in lung but not in heart tissue homogenates (Supplemental Fig.2E; the residual Trx2 protein detected in Trx2-cKO was from other cell types such as endothelium other than cardiomyocytes); 4) finally, immunoblotting with anti-Trx2 antibody confirmed the deficiency of Trx2 protein expression in cardiomyocytes isolated from Trx2-cKO hearts but not in vascular endothelial cells (Supplemental Fig.2F).

$Trx2^{lox/lox}$ mice were viable and developmentally normal with similar cardiac function to WT C57BL/6 mice at birth. However, Trx2-cKO mice had 100% mortality by 4 months of

age, with survival declining rapidly starting at 3 months of age (Fig.2A). Longitudinal echocardiogram analyses of Trx2-cKO at 1, 2 and 3 months after birth revealed a severe dilated cardiomyopathy with a significant reduction in LV fractional shortening (%FS) in Trx2-cKO compared to control $Trx2^{lox/lox}$ hearts, with a progressive decline in LV function from 1–3 months (Fig.2B–C). Trx2-cKO mice also exhibited progressive increases in LV systolic and diastolic dimensions from 1–3 months (Fig.2D–E). At 3 months of age the Trx2-cKO mice had significantly reduced LV peak systolic pressure (Fig.2F), reduced rates of left ventricular pressure increase (+dP/dt) and pressure decrease (−dP/dt) (Fig.2G), indicative of LV contractile dysfunction.

Structural and molecular analyses of dilated cardiomyopathy in Trx2-cKO mice

To determine the structural basis for the abnormal cardiac function caused by Trx2 deletion, we performed gross, histological and ultrastructural analyses of Trx2-cKO hearts at 1, 2 and 3 months after birth. Trx2-cKO mice had age-dependent increases in heart weight (but not in body weight) and in the ratio of heart weight to body weight, indicating a cardiac hypertrophic response (Fig.3A–C). Trx2-cKO mice also had elevated lung/body weight ratio compared to the control group at 3 months (Fig.3D), indicative of pulmonary edema caused by cardiac defects. Gross pathological changes were also apparent in the hearts of Trx2-cKO mice, including marked atrial and ventricular dilation. H&E staining of sagittal cross sections revealed that Trx2-cKO had marked four-chamber enlargement (Fig.3E). Quantitative analyses of cardiomyocyte cross-section area visualized by H&E (Fig.3F) and wheat germ agglutinin (WGA; Fig.3G) staining revealed age-dependent increases in cell size in Trx2-cKO hearts (Fig.3H). WGA staining for cell surfaces also detected capillaries in the myocardium, but the ratio of capillary/myocyte (~5:1) was not significantly altered in Trx2-cKO heart. Trx2-cKO hearts also had age-dependent increases in interstitial fibrosis in both the atria and ventricles as detected using Mason's Trichrome staining (Fig.3I and Supplemental Fig.3). Taken together, these data suggest Trx2 is required for the maintenance of normal cardiac structure and function during early cardiac growth.

To characterize the molecular changes associated with the dilated cardiomyopathy and heart failure phenotype, we performed gene expression profiling. Six pairs of heart tissues from WT and Trx2-cKO mice at 3 months of age were subjected to NanoString analysis of gene expression. This molecular analysis revealed striking upregulation/downregulation of genes that are well established markers of human heart failure and which are highly consistent with the DCM phenotype observed in the Trx2-cKO mice (Fig.3J). Among the genes with significant dysregulation in Trx2-cKO included classic markers of heart failure, including ANP and BNP (the highest induced up-regulated genes, increased by ~17 and ~10-fold, respectively). There was also clear induction of hypertrophic fetal gene reprograming, with cardiac deletion of Trx2 resulting in a ~4-fold upregulation of βMHC (withconcomitant 4-fold downregulation of αMHC) and a ~5-fold increase in expression of cardiac α-actin. There was also significant upregulation of pro-fibrotic genes including TIMP-1 (increased by ~7-fold), periostin (increased by ~5-fold), TGF-β2 (increased by ~4-fold), PAI-1 (increased by ~3-fold), and LOX (increased by ~3-fold) consistent with the fibrotic myocardium of the Trx2-cKO mice at 3 months (Supplemental Fig 3). In contrast, there was a consistent downregulation of genes regulating Ca^{2+} handling and contractility. These

included the α1-adrenergic receptor (gene expression reduced by ~11-fold, the most downregulated gene) the β1 adrenergic receptor (reduced by ~3-fold,) phospholamban (reduced by ~6-fold) the rryanodine receptor-2 (RYR2, reduced by ~5-fold), and the sarco/endoplasmic reticulum Ca^{2+}-ATPase (SERCA2A, reduced by ~5-fold). There was also reduced expression of ion-channels which regulate the cardiac action potential, including the voltage-gated potassium channels Kv4.2 (reduced by ~5-fold) and Kv4.3 (reduced by ~3-fold), and the hyperpolarization-activated cyclic nucleotide-gated cation channel-4 (HCN4) (reduced by 5-fold). As expected, with cardiac-specific knockout of a key anti-oxidant enzyme, a number of redox signaling genes were significantly perturbed in the Trx2-cKO heart. These included a 2.5-fold increase in expression of NAPDH oxidase 4 (NOX4) and a decrease in expression of antioxidant genes, including mitochondrial SOD2 (reduced by ~5-fold), mitochondrial ALDH2 (reduced by ~3-fold) and glutathione-s-transferase (reduced by ~2-fold). Nanosting analysis revealed dysregulation of a number of apoptotic genes, with ~2 fold increase in the pro-apoptotic Fas-Ligand and a decrease in anti-apoptotic BCl211 (reduced by ~4-fold). Notably, there was a significant 4-fold decrease in the expression of the mitochondrial biosynthesis genes peroxisome proliferator-activated receptor gamma-coactivator (PGC-1α) and the peroxisome proliferator-activated receptor alpha (PPARα)[25, 26]. Taken together, these changes in gene expression provide molecular insight into the pathological processes (oxidative stress, apoptosis, fibrosis, electrical remodeling, contractile dysfunction) which occur in the myocardium as a consequence of cardiac-specific deletion of Trx2, and are consistent with the constellation of changes in myocardial structure, metabolism, and electrophysiology which occur in human heart failure[1, 2].

Mitochondria in Trx2-cKO hearts exhibit disrupted integrity and reduced function

To test our hypothesis that Trx2 exerts its endogenous cardioprotective function by preserving mitochondrial integrity and function, we measured mitochondrial structure, mitochondrial DNA copy and mass, mitochondrial function (ATP production and oxygen consumption rate) in WT and Trx2-cKO hearts. Mitochondrial integrity was first determined by ultrastructural analyses, using electron microscopy, in sections from the control and Trx2-cKO mouse hearts (Fig. 4A–B). In normal myocardium, mitochondria were aligned in well-preserved rows between the longitudinally oriented cardiac myofibrils. Although the abundance of mitochondria in Trx2-cKO appeared not be significantly altered, loss of Trx2 at 1 month of age resulted in disorganized mitochondrial arrays and aggregates of swollen mitochondria with mild lysis of the cristae (Fig.4A with higher power on the right). At 3 months of age, there was evidence of extensive damage to cardiac mitochondria and disrupted cristae were detected in Trx2-cKO hearts (Fig.4B). Measurement of mitochondrial DNA copy number (mtDNA) by quantitative PCR suggest that Trx2 deficiency in mouse hearts caused no significant change in mtDNA copy number at 1–2 months of age, and only slight (76%) reduction at 3-months (Fig.4C). Cytochrome C oxidases (COX) are located in the inner mitochondrial membrane and function as an important terminal enzyme complex of the mitochondrial electron transport chain. COX protein expression can be used as an indicator for both mitochondrial mass and function[27]. There was a dramatic reduction in protein expression of both COX1 and COX4, which were reduced in an age-dependent manner in Trx2-cKO hearts. By 3 months of age, COX1 protein in the Trx2-cKO had declined to only 7.5% of control, whereas COX4 had declined to 37.5% (Fig.4D with

quantification in 4E). The mitochondrial electron transport chain (ETC) consumes oxygen by oxidative phosphorylation to form cellular energy in the form of ATP. Therefore, we measured ATP content as a global readout of mitochondrial function[28, 29]. In Trx2-cKO hearts, ATP content was significantly impaired, as early as 1 month of age (Fig.4F) and progressively declined to reach only 35% of WT hearts at 3 months. We further measured oxygen consumption rate (OCR) in cardiomyocytes isolated from WT and Trx2-cKO at one month of age. Trx2 deletion decreased the basal respiration, ATP coupler response (Oligomycin) and ETC accelerator response (FCCP) (Fig.4G). Addition of succinate substrate enhanced OCR in WT but not in Trx2-deficient cardiomyocytes (Fig.4H vs. 4G). These morphological and biochemical data indicate that Trx2 is essential to maintain mitochondrial integrity and function in the heart and that Trx2 deletion results in catastrophic loss of key mitochondrial integrity, leading to mitochondrial swelling, ultrastructural derangement and reduced respiration and ATP production.

Cardiac-specific Trx2 deletion induces mitochondrial ROS production, ASK1 activation, and promotesapoptosis in the myocardium

Oxidative stress and cellular apoptosis have been strongly implicated in the progression of hypertrophy and heart failure[3–6, 30, 31]. We reasoned that disrupted mitochondrial integrity and function induced by Trx2 deletion would promote ROS generation and cellular apoptosis. We therefore examined Trx2-cKO hearts for oxidative stress levels using the ROS probe di-hydroethidium (DHE) and measured apoptosis using the TUNEL assay. Loss of cardiac Trx2 resulted in age-dependent increases both in apoptosis (Fig.5A–C) and oxidative stress (Fig.5D–E). To confirm that cardiac-specific deletion of Trx2 indeed reduced Trx2 activity in cardiac mitochondria, we determined Trx2 activity and measured ROS in mitochondria isolated from WT and Trx2-cKO hearts. While both Trx2 and TrxR2 (but not the cytosolic protein GAPDH), were detected in mitochondria isolated from WT hearts. Trx2 protein expression and activity were almost completely absent in mitochondria isolated from Trx2-cKO hearts at 1 month of age (Fig.5 F–G). Any residual Trx2 protein expression/activity observed in the Trx2-cKO likely comes from Trx2 expression in non-cardiomyocyte cells (i.e. fibroblasts, endothelial cells or vascular smooth muscle cells which do not have Trx2 deletion driven by the MHC-Cre promoter. To confirm that Trx2 deletion resulted in increased ROS, we measured rates of ROS generation in WT and Trx2-cKO mitochondria using the mitochondrial-specific probe MitoSOX. As expected, ROS generation was significantly enhanced in Trx2-cKO mitochondria (Increased by 2.7-fold in Trx2-cKO mitochondria compared with WT control, n=3, $p<0.01$, Fig.5H), confirming that Trx2 deletion directly promotes mitochondrial ROS generation.

We next investigated both mitochondrial and cytosolic antioxidant pathways for evidence of a compensatory response to Trx2 deletion at 1 and 3 months of age. At 1 month, Trx2-cKO did not cause significant alterations in expression of anti-oxidant proteins, including cytosolic Trx1 and glutathione peroxidase 1 (Gpx1), mitochondrial TrxR2 and superoxide dismutase-2 (SOD2). However, by 3 months of age, there were elevations in expression of the mitochondrial anti-oxidant proteins TrxR2 (2.8-fold increase, n=6) and SOD2 (1.7-fold increase, n=6) in the Trx2-cKO myocardium, (Fig.5I), suggesting the involvement of a compensatory mechanism to account for increased mitochondrial ROS generation. The weak

increase in mitochondrial SOD2 protein level was in contrast to the 5-fold reduction in SOD2 mRNA level measured by gene expression, indicating that mitochondrial SOD2 protein is likely regulated at the post-transcriptional level. We also measured glutathione levels as an indicator of global thio-redox status, and found that total glutathione and ratios of GSSG:GSH were not significantly altered in Ctrl and Trx2-cKO heart tissues (Supplemental Fig.4B). These data suggest that mitochondrial, but not cytosolic, anti-oxidant pathways were specifically altered to compensate for lack of Trx2.

We next investigated potential signaling mechanisms by which Trx2 deletion, and mitochondrial ROS generation, promote apoptosis in the myocardium. We have previously shown that Trx2 (in its reduced form) directly binds to mitochondrial-localized ASK1 and inhibits ASK1-mediated apoptosis[14]. Oxidation of Trx2, or Trx2 deletion, liberates ASK1 from Trx2 binding, and results in ASK1 autophosphorylation and activation, resulting in induction of mitochondrial-dependent cell death mediated *via* caspase-3 cleavage, in a mechanism that is independent of JNK[14]. In agreement with our previous study, ASK1 protein was detected by western blot in cardiac mitochondria from WT, but ASK1 level was increased in mitochondria from the Trx2-cKO heart at 1 month (Fig.5F). Furthermore, Trx2-cKO strongly induced ASK1 autophosphorylation at Thr845, (a marker of ASK1 activity), which was evident as early as 1 month of age and persisted through 3 months of age (Fig. 5J, top panels), and occurred concomitantly with the increase in ROS observed in Fig.5D–E. ROS-dependent phosphorylation of JNK and caspase-3 activation were only apparent at the late stage (3-months of age) in Trx2-cKO heart (Fig.5J). These data suggest that mitochondrial dysfunction and activation of ASK1 may be an early event in the development of cardiac dysfunction induced by Trx2 deletion.

Deletion of Trx2 in cardiomyocytes induces ASK1 activation, mitochondrial dysfunction with increased cellular ROS and apoptosis

Having established that cardiac-specific deletion of Trx2 increased ASK1 activity in the myocardium early in DCM disease progression, we explored the direct effect of Trx2 deletion on ASK1 activity in isolated cardiomyocytes. Neonatal cardiomyocytes were isolated from $Trx2^{lox/lox}$ mice and then infected with Cre-expressing adenovirus to specifically delete Trx2 *in vitro*. Tropomyosin staining indicated that >90% of cells isolated from neonatal heart were cardiomyocytes, which could be efficiently infected by Cre-expressing adenoviruses. Trx2 protein was not detected in cardiomyocytes expressing Cre, as examined by immunostaining (Supplemental Fig.5). Trx2 deletion resulted in a ~3-fold increase in ASK1 phosphorylation, which occurred without significant increases in JNK phosphorylation (Fig.6A with quantifications in 6B). These data are consistent with our previous observation that Trx2-ASK1 regulates mitochondrial apoptosis, independent of JNK phosphorylation[14]. Trx2 deletion also resulted in significant mitochondrial membrane depolarization in isolated cardiomyocytes, as demonstrated by the significant reduction in red/green JC-1 ratio (**6C** with quantifications in **6D**). As an intact $\Delta\Psi m$ is required for ATP generation through ATP synthase, this result is consistent with the reduction of ATP production observed in Trx2-cKO heart (Fig.4A). As observed in the Trx-2cKO heart, Trx2 deletion in the cardiomyocyte also led to an ~3-fold increase in mitochondrial ROS generation (Fig.6E with quantifications in 6F), and resulted in cardiomyocyte apoptosis (Fig.

6G with quantifications in 6H), as measured using a mitochondrial ROS probe MitoSOX and TUNEL assays, respectively.

Inhibition of ASK1 prevents Trx2 deletion-induced mitochondrial dysfunction, ROS accumulation, and apoptosis in cardiomyocytes

Having observed that Trx2 deletion robustly induced ASK1 phosphorylation in both the myocardium (Fig.5J) and in isolated cardiomyocytes (Fig.6A), we determined whether ASK1 activity was necessary to mediate the cellular consequences of Trx2 deletion in the cardiomyocyte. GS-444217 is a selective, small molecule inhibitor of ASK1 that was synthesized at Gilead Sciences Inc. GS-444217 at 1 μM inhibited >90% cellular ASK1 autophosphorylation induced by ASK1 overexpression (Fig.7A–B), and completely inhibited ASK1-dependent phosphorylation of p38, induced by either ASK1 overexpression, or treatment with 100 μM H_2O_2 (Supplemental Fig.6). In Trx2-deficient cardiomyocytes with Trx2 deleted by adenoviral Cre infection, treatment with 1 μM GS-444217 significantly reduced (by 2.6-fold) the Trx2-deletion induced increase in ASK1 phosphorylation (Fig.7C, with quantification in 7D) and caspase-3 cleavage (Fig.7E with quantification in 7F). Further, ASK1 inhibition significantly attenuated both mitochondrial ROS production (80% inhibition) detected by MitoSOX fluorescence (Fig.7G with quantification in Fig.7H) and cardiomyocyte apoptosis (67% inhibition) detected by TUNEL staining (Fig.7I with quantifications in Fig.7J).

We next used an alternative cardiomyocyte cell line (rat H9C2) to confirm the role of the Trx2-ASK1 axis in regulating cardiomyocyte viability. Knockdown of Trx2 in H9C2 by siRNA induced ASK1 phosphorylation (increased by ~3-fold), without activating JNK or p38, consistent with the data using MHC-Cre Trx2 deletion in murine cardiomyocytes. Furthermore, 1μM GS-444217 inhibited Trx2 knockdown-induced ASK1 activity (60% inhibition of ASK1 phosphorylation), abolised mitochondrial ROS generation and prevented Trx2-knockdown-induced apoptosis to control levels (apoptotic cells increased from ~5% with ctrl siRNA to ~12% in trx2 sIRNA and reduced back to ~5% in Trx2siRNA+ 1μM GS-444217) (Supplemental Fig.7C–E). These cellular data (obtained using cardiomyocyte cell lines from two different species), demonstrate that ASK1 activity is required for Trx2 deletion-induced mitochondrial dysfunction, ROS production and cardiomyocyte apoptosis, suggesting that ASK1 is a critical effector of mitochondrial-dependent cardiomyocyte cell death induced by Trx2 deletion.

ASK1 inhibition attenuates the development of dilated cardiomyopathy in Trx2-cKO mice

Finally, we determined whether inhibition of ASK1 with GS-444217, could attenuate the development of cardiac dysfunction and LV-remodeling induced by cardiac Trx2 deficiency in mice. WT control and Trx2-cKO mice were given GS-444217 first by oral gavage (30 mg/kg, once a day, from P10 to P27) followed by diet chow containing GS-444217. Cardiac function and dilated cardiomyopathy phenotype were determined by echocardiogram (performed monthly from 1–4 months) and also by histological and biochemical analyses (performed at 3 months). GS-444217 treatment had no significant effects on body weight, cardiac function, or survival in WT control mice (Fig.8A–B). Importantly, ASK1 inhibition significantly reduced cardiac dysfunction and LV dilation and greatly prolonged the life-

span of Trx2-cKO mice, whose median survival increased by 40 days (n=15, p<0.001) (Fig. 8A). GS-444217 significantly attenuated the progressive decline in LV fractional shortening observed in the Trx2-cKO mice from 1–3 months of age (Fig.8B). At 3 months of age, GS-444217 treatment improved %FS in the Trx2-cKO group by 52%, compared to vehicle-treated Trx2-cKO mice (39% FS in the vehicle Trx2-cKO group compared to 18% FS in the GS-444217 treated Trx2-cKO group, n=10, p<0.001). ASK1 inhibition also significantly attenuated LV dilation induced by cardiac-specific deletion of Trx2 (Fig.8.B). At 3 months of age, GS-444217 reduced the increase in LV Vol(d) and the LV Vol(s) from 125 μl and 78 μl in the vehicle Trx2-cKO group compared to 75 μl and 22 μl, respectively, in the GS-444217 treated Trx2-cKO group, n=10, p<0.01) (Fig.8B). The effect of ASK1 inhibition on the hypertrophic phenotype of Trx2-cKO heart was confirmed by histological analysis of cardiomyocyte area (cardiomyocyte area was increased by 2.8-fold in Trx2-cKO vehicle, compared to WT control, and by only 1.8-fold in Trx2-cKO GS-444217 group, n=10, p<0.01, Supplemental Fig 8A) and analysis of ANP gene expression (GS-444217 treatment reduced ANP expression by 50% compared to Trx2-cKO vehicle hearts, Supplemental Fig. 8B). As observed in cultured cardiomyocytes with Trx2 gene deletion, GS-444217 attenuated ROS production (DHE staining in Trx2-cKO myocardium was reduced by 64% with GS-444217, compared to vehicle-treated mice, n=10, p<0.01) and apoptosis (TUNEL staining in Trx2-cKO myocardium was reduced by 55% with GS-444217, compared to vehicle-treated mice, n=10, p<0.05) in the myocardium of Trx2-cKO mice (Fig.8C with quantifications in Supplemental Fig.8C–D). Consistent with results observed in cardiomyocytes, GS-444217 also inhibited the Trx2 deletion-induced activation of ASK1 (p-ASK1 induced by Trx2-cKO was reduced by 60% with GS-444217 (n=5, p<0.05), and significantly reduced caspase-3 cleavage by 50% with GS-444217, (n=10, p<0.01) In addition, GS-444217 also attenuated Prx3 dimerization induced by Trx2-cKO (reduced by 86% with GS-444217, compared with vehicle, n=5, p<0.05) (Representative Western Blots in Fig.8D, with quantification in Fig.8E).

DISCUSSION

In the present study, we generated a mouse line where Trx2 was specifically deleted in cardiomyocytes. Using this model, we have demonstrated, for the first time, that the mitochondrial redox protein Trx2 is essential in preserving cardiac function by maintaining mitochondrial integrity, suppressing ROS production, and preventing ASK1-dependent apoptosis. Mice with a targeted, cardiac-specific deletion of Trx2 (Trx2-cKO) develop a progressive dilated cardiomyopathy, characterized by heart chamber dilation, wall thinning, interstitial fibrosis and impaired contractile function, culminating in heart failure and death by 4 months of age. Histological and biochemical analysis of Trx2-cKO hearts from 1 to 3 months indicate that Trx2 deletion induces a progressive derangement of mitochondrial structure and function, resulting in mitochondrial swelling, reduced respiration, and concomitant reduction in ATP generation, accompanied by increased ROS production and cellular apoptosis. Cardiomyocytes deficient in Trx2 displayed a similar cellular phenotype, suggesting that the cardioprotective function of Trx2 observed in the heart is intrinsic to the cardiomyocyte. Mechanistic analyses indicate marked increases in ASK1 signaling and mitochondrial damage occurring early in the progression of cardiac dysfunction in the Trx2-

cKO heart. Increased myocardial ASK1 activity is sustained and appears to play a key role in driving pathological cardiac remodeling induced by Trx2-cKO as inhibition of ASK1 prevents Trx2 deletion-induced ROS production and apoptosis in cardiomyopcytes, and slows the progression of dilated cardiomyopathy and heart failure *in vivo*. Of potential clinical relevance, there is evidence that dysregulation of the Trx2-ASK1 signaling axis also occurs in human DCM, as LV biopsies from patients with end-stage idiopathic dilated cardiomyopathy have reduced Trx2 expression, increased ASK1 phosphorylation, and increased caspase-3 cleavage. Taken together, our studies have established Trx2 as an essential antioxidant enzyme in the heart, whose activity is critically required for suppressing ROS-induced ASK1 activation and preventing maladaptive LV remodeling.

Both the cytosolic Trx1/TrxR1 and the mitochondrial Trx2/TrxR2 systems are implicated in protecting against the pathogenesis of cardiac dysfunction[8, 32]. Exogenous Trx1 has cardioprotective effects in models of myocardial infarction[33, 34] andTrx1 transgenic mouse hearts overexpressing Trx1 are resistant to ischemia/reperfusion[35]. Conversely, transgenic mice with cardiac-specific overexpression of a dominant negative mutant (C32S/C35S) of Trx1 develop cardiac hypertrophy[36], but do not develop dilated cardiomyopathy or heart failure. Mechanistic studies have suggested that Trx1 modulates the redox modification and nucleocytoplasmic shuttling of class II histone deacetylases, master regulators of cardiac hypertrophy[37]. Our current study suggests that mitochondrial Trx2 in heart has distinct functions from the cytosolic Trx1. Here, we found that cardiac-specific ablation of Trx2 induces severe dilated cardiomyopathy, resulting in heart failure. Consistent with our findings, TrxR2, an enzyme that is critical for Trx2 activity, is also associated with dilated cardiomyopathy[15]. In a rat model of cardiac ischemia/reperfusion injury, administration of the TrxR2 inhibitor auranofin, significantly impairs post-ischemic recovery of function with increased cardiac apoptosis[38]. Similarly, cardiac-specific deletion of TrxR2 in mice results in increased infarct size and increased sensitivity to mitochondrial permeability transition[39]. These data suggest that mitochondrial TrxR2, like Trx2, is essential for endogenous cardioprotection. Recent clinical studies indicate that loss-of-function genetic mutations in the TrxR2 gene, leading to reduced flavin-adenine dinucleotide binding, are associated with dilated cardiomyopathy[20]. It is not yet known whether any genetic mutations or polymorphisms of the Trx2 gene are also associated with dilated cardiomyopathy in humans. Nevertheless, our data demonstrate that human hearts from patients with end-stage idiopathic cardiomyopathy have reduced Trx2 expression, concomitant with increased ASK1 activity, highlighting the importance of Trx2 in preserving heart function in humans. The mechanism(s) responsible for Trx2 downregulation in human cardiomyopathy and heart failure are unknown and need to be investigated further. We have recently shown that the TrxR2 inhibitor auranofin reduces Trx2 protein level (but not its mRNA), suggesting that TrxR2 activity is required for Trx2 protein stability and that oxidized Trx2 is more accessible for degradation[40].

Analyses of cardiac function, histology and gene expression demonstrate that the Trx2-cKO mice feature many of the pathological processes (oxidative stress, apoptosis, fibrosis, electrical remodeling, contractile dysfunction) which occur in human heart failure. Thus, Trx2-cKO may provide a useful preclinical model to examine the pathogenesis and

molecular mechanisms of dilated cardiomyopathy and heart failure. Among genes with significant changes in the Trx2-cKO hearts detected by gene expression profiling were increases in well established markers of cardiac hypertrophy, heart failure, and cardiac fibrosis. Conversely, genes which encode proteins that regulate the cardiomyocyte action potential and Ca^{2+} handling/contraction were substantially downregulated in the Trx-cKO mice. It is not clear, however, which of these changes in gene expression occur as a direct result of cardiac-specific ablation of Trx2, and which occur as a consequence of the heart failure phenotype. Nevertheless, the molecular adaptations observed in the LV of the Trx2-cKO mice are highly consistent with those previously reported in human heart failure and in other preclinical models of DCM and heart failure.

Trx2 is a mitochondrial antioxidant, which exerts its endogenous cardioprotective function by protecting against excessive mitochondrial ROS, thus preserving mitochondrial integrity and function. The data herein indicate that the severe derangement of mitochondrial structure and function most likely contributes directly to the development of dilated cardiomyopathy in the Trx2-cKO mice. Trx2-cKO hearts had a progressive loss of mitochondrial integrity and function, as measured by mitochondrial copy number, mass, ultrastructure, mitochondrial permeability and ATP production. Electron microscopic analyses revealed that mitochondria are parallel to the longitudinal axis of oriented intermediate filaments in normal murine hearts. The close proximity of well-aligned rows of mitochondria to the longitudinally oriented cardiac myofibrils is essential to provide a rapid and constant supply of ATP for contractile function[41]. However, mitochondria in Trx2-cKO heart are spread irregularly between disorganized myofibrils. Mitochondria in Trx2-cKO heart also appear swollen with numerous disrupted cristae. These morphological alterations are accompanied by the disruption of the mitochondrial membrane potential, reduced protein expression of the mitochondrial electron transport chain complexes COX1 and COX4, as well as significantly reduced ATP production. The structural and functional alterations of mitochondria observed in Trx2-cKO hearts likely contribute to the reduced contractile force in Trx2-cKO mice with dilated cardiomyopathy. Loss of mitochondrial COX1/4 proteins also likely affects the capacity of mitochondria to collect electrons, and to transfer electrons from cytochrome C to molecular oxygen, leading to increases in electron leakage and further ROS production. Trx2, via mitochondrial peroxidase Prx3, can also directly scavenge ROS (H_2O_2). A shift of Prx3 from active monomers to inactive dimers in Trx2-cKO heart may also contribute further to ROS production.

One of the major findings in this work is that Trx2 deletion in the heart triggers a cascade of mitochondrial ROS production, ASK1 activation and cellular apoptosis, which promotes progressive maladaptive LV remodeling and cardiac dysfunction in Trx2-cKO mice (Supplemental Fig.9). A surprising finding in the current study is that ASK1 activity is markedly increased in the early stages of DCM disease progression and precedes mitochondrial damage, cellular apoptosis and cardiac dysfunction in the Trx2-cKO heart. Additionally, ASK1 was detected in mitochondria isolated from the WT hearts, and mitochondrial ASK1 level was increased by Trx2 deletion.. Importantly, treatment with an ASK1-specific inhibitor blocked ROS production, mitochondrial dysfunction and cellular apoptosis induced by either Trx2 deletion or siRNA knockdown in cardiomyocytes, confirming that ASK1 is a key mediator of cardiomyocyte injury induced by Trx2 deletion.

We have previously reported that Trx2 can directly bind to and inhibit mitochondrial-localized ASK1, and inhibit mitochondrial-dependent apoptosis, independent from JNK phosphorylation[14]. Our data in the current study suggest that ASK1 activation, mitochondrial dysfunction and ROS production are three interdependent events which may form a vicious positive-feedback cycle, which promote cardiomyocyte cell death (see Supplemental Fig.9 for a model): Deletion or knockdown of Trx2 in cardiomyocytes increases ASK1 activity, and promotes mitochondrial dysfunction, ROS production and apoptosis. Importantly, these Trx2 deletion-induced effects in cardiomyocytes could be completely attenuated by ASK1 inhibition, demonstrating a causal role for ASK1 as a critical effector of mitochondrial-dependent cardiomyocyte cell death induced by Trx2 deletion.

The role of apoptosis in the development of dilated cardiomyopathy has been previously demonstrated using an inducible expression of an apoptotic protein in the mouse heart[42, 43]. Inducible expression of caspase-8 in heart confers cardiomyocyte apoptosis at a low rate (0.023%) which is sufficient to cause a lethal, dilated cardiomyopathy within 8–24 weeks. Interestingly, this time course for dilated cardiomyopathy and lethality is close to that observed in the Trx2-cKO mice. These data indicate that cardiomyocyte apoptosis may represent a common mechanism for the progression of dilated cardiomyopathy and heart failure. Importantly, inhibition of ASK1 could prevent maladaptive LV remodeling, and rescue the cardiac dysfunction in Trx2-cKO mice, similar to the rescue observed by ROS-scavengers or caspase inhibitors in other models of heart failure[42, 43]. Recent reports have demonstrated that inhibition of ASK1 could also reduce myocardial infarct size in rat and mouse models of ischemia/reperfusion[44, 45]. Our data provides the first report that inhibition of ASK1 is a potential therapeutic strategy for the treatment of dilated cardiomyopathy and heart failure.

Supplementary Material

Refer to Web version on PubMed Central for supplementary material.

Acknowledgements

We thank Kevin Xu for technical support.

Funding Sources: This work was supported by NIH grants R01 HL085789 and R01 HL109420.

References

1. Haider AW, Larson MG, Benjamin EJ, Levy D. Increased left ventricular mass and hypertrophy are associated with increased risk for sudden death. J Am Coll Cardiol. 1998; 32:1454–1459. [PubMed: 9809962]
2. Heineke J, Molkentin JD. Regulation of cardiac hypertrophy by intracellular signalling pathways. Nat Rev Mol Cell Biol. 2006; 7:589–600. [PubMed: 16936699]
3. Mann DL, Bristow MR. Mechanisms and models in heart failure: the biomechanical model and beyond. Circulation. 2005; 111:2837–2849. [PubMed: 15927992]
4. Murdoch CE, Zhang M, Cave AC, Shah AM. NADPH oxidase-dependent redox signalling in cardiac hypertrophy, remodelling and failure. Cardiovasc Res. 2006; 71:208–215. [PubMed: 16631149]

5. Sorescu D, Griendling KK. Reactive oxygen species, mitochondria, and NAD(P)H oxidases in the development and progression of heart failure. Congest Heart Fail. 2002; 8:132–140. [PubMed: 12045381]

6. Giordano FJ. Oxygen, oxidative stress, hypoxia, and heart failure. J Clin Invest. 2005; 115:500–508. [PubMed: 15765131]

7. Crow MT, Mani K, Nam YJ, Kitsis RN. The mitochondrial death pathway and cardiac myocyte apoptosis. Circ Res. 2004; 95:957–970. [PubMed: 15539639]

8. Ago T, Sadoshima J. Thioredoxin and ventricular remodeling. J Mol Cell Cardiol. 2006; 41:762–773. [PubMed: 17007870]

9. Holmgren A. Antioxidant function of thioredoxin and glutaredoxin systems. Antioxid Redox Signal. 2000; 2:811–820. [PubMed: 11213485]

10. Santos CX, Anilkumar N, Zhang M, Brewer AC, Shah AM. Redox signaling in cardiac myocytes. Free Radic Biol Med. 2011; 50:777–793. [PubMed: 21236334]

11. Lee S, Kim SM, Lee RT. Thioredoxin and Thioredoxin Target Proteins: From Molecular Mechanisms to Functional Significance. Antioxid Redox Signal. 2013; 18:1165–1207. [PubMed: 22607099]

12. Pober JS, Min W, Bradley JR. Mechanisms of Endothelial Dysfunction, Injury, and Death. Annu Rev Pathol. 2009; 4:71–95. [PubMed: 18754744]

13. Hatai T, Matsuzawa A, Inoshita S, Mochida Y, Kuroda T, Sakamaki K, Kuida K, Yonehara S, Ichijo H, Takeda K. Execution of apoptosis signal-regulating kinase 1 (ASK1)-induced apoptosis by the mitochondria-dependent caspase activation. J Biol Chem. 2000; 275:26576–26581. [PubMed: 10849426]

14. Zhang R, Al-Lamki R, Bai L, Streb JW, Miano JM, Bradley J, Min W. Thioredoxin-2 inhibits mitochondria-located ASK1-mediated apoptosis in a JNK-independent manner. Circ Res. 2004; 94:1483–1491. [PubMed: 15117824]

15. Conrad M, Jakupoglu C, Moreno SG, Lippl S, Banjac A, Schneider M, Beck H, Hatzopoulos AK, Just U, Sinowatz F, Schmahl W, Chien KR, Wurst W, Bornkamm GW, Brielmeier M. Essential role for mitochondrial thioredoxin reductase in hematopoiesis, heart development, and heart function. Mol Cell Biol. 2004; 24:9414–9423. [PubMed: 15485910]

16. Nonn L, Williams RR, Erickson RP, Powis G. The absence of mitochondrial thioredoxin 2 causes massive apoptosis, exencephaly, and early embryonic lethality in homozygous mice. Mol Cell Biol. 2003; 23:916–922. [PubMed: 12529397]

17. Tanaka T, Hosoi F, Yamaguchi-Iwai Y, Nakamura H, Masutani H, Ueda S, Nishiyama A, Takeda S, Wada H, Spyrou G, Yodoi J. Thioredoxin-2 (TRX-2) is an essential gene regulating mitochondria- dependent apoptosis. Embo J. 2002; 21:1695–1703. [PubMed: 11927553]

18. Jakupoglu C, Przemeck GK, Schneider M, Moreno SG, Mayr N, Hatzopoulos AK, de Angelis MH, Wurst W, Bornkamm GW, Brielmeier M, Conrad M. Cytoplasmic thioredoxin reductase is essential for embryogenesis but dispensable for cardiac development. Mol Cell Biol. 2005; 25:1980–1988. [PubMed: 15713651]

19. Matsui M, Oshima M, Oshima H, Takaku K, Maruyama T, Yodoi J, Taketo MM. Early embryonic lethality caused by targeted disruption of the mouse thioredoxin gene. Dev Biol. 1996; 178:179–185. [PubMed: 8812119]

20. Sibbing D, Pfeufer A, Perisic T, Mannes AM, Fritz-Wolf K, Unwin S, Sinner MF, Gieger C, Gloeckner CJ, Wichmann HE, Kremmer E, Schafer Z, Walch A, Hinterseer M, Nabauer M, Kaab S, Kastrati A, Schomig A, Meitinger T, Bornkamm GW, Conrad M, von Beckerath N. Mutations in the mitochondrial thioredoxin reductase gene TXNRD2 cause dilated cardiomyopathy. Eur Heart J. 2011; 32:1121–1133. [PubMed: 21247928]

21. Zhang H, Luo Y, Zhang W, He Y, Dai S, Zhang R, Huang Y, Bernatchez P, Giordano FJ, Shadel G, Sessa WC, Min W. Endothelial-specific expression of mitochondrial thioredoxin improves endothelial cell function and reduces atherosclerotic lesions. Am J Pathol. 2007; 170:1108–1120. [PubMed: 17322393]

22. Dai S, He Y, Zhang H, Yu L, Wan T, Xu Z, Jones D, Chen H, Min W. Endothelial-specific expression of mitochondrial thioredoxin promotes ischemia-mediated arteriogenesis and angiogenesis. Arterioscler Thromb Vasc Biol. 2009; 29:495–502. [PubMed: 19150880]

23. Lyons GE, Schiaffino S, Sassoon D, Barton P, Buckingham M. Developmental regulation of myosin gene expression in mouse cardiac muscle. J Cell Biol. 1990; 111:2427–2436. [PubMed: 2277065]
24. Cox AG, Winterbourn CC, Hampton MB. Mitochondrial peroxiredoxin involvement in antioxidant defence and redox signalling. Biochem J. 2010; 425:313–325.
25. Wu Z, Puigserver P, Andersson U, Zhang C, Adelmant G, Mootha V, Troy A, Cinti S, Lowell B, Scarpulla RC, Spiegelman BM. Mechanisms controlling mitochondrial biogenesis and respiration through the thermogenic coactivator PGC-1. Cell. 1999; 98:115–124. [PubMed: 10412986]
26. Martin OJ, Lai L, Soundarapandian MM, Leone TC, Zorzano A, Keller MP, Attie AD, Muoio DM, Kelly DP. A role for peroxisome proliferator-activated receptor gamma coactivator-1 in the control of mitochondrial dynamics during postnatal cardiac growth. Circ Res. 2014; 114:626–636. [PubMed: 24366168]
27. Srinivasan S, Avadhani NG. Cytochrome c oxidase dysfunction in oxidative stress. Free Radic Biol Med. 2012; 53:1252–1263. [PubMed: 22841758]
28. Dedkova EN, Blatter LA. Measuring mitochondrial function in intact cardiac myocytes. J Mol Cell Cardiol. 2012; 52:48–61. [PubMed: 21964191]
29. Brand MD, Nicholls DG. Assessing mitochondrial dysfunction in cells. Biochem J. 2011; 435:297–312. [PubMed: 21726199]
30. Byrne JA, Grieve DJ, Cave AC, Shah AM. Oxidative stress and heart failure. Arch Mal Coeur Vaiss. 2003; 96:214–221. [PubMed: 12722552]
31. Grieve DJ, Byrne JA, Cave AC, Shah AM. Role of oxidative stress in cardiac remodelling after myocardial infarction. Heart Lung Circ. 2004; 13:132–138. [PubMed: 16352183]
32. Ago T, Sadoshima J. Thioredoxin1 as a negative regulator of cardiac hypertrophy. Antioxid Redox Signal. 2007; 9:679–687. [PubMed: 17419666]
33. Tao L, Gao E, Bryan NS, Qu Y, Liu HR, Hu A, Christopher TA, Lopez BL, Yodoi J, Koch WJ, Feelisch M, Ma XL. Cardioprotective effects of thioredoxin in myocardial ischemia and reperfusion: role of S-nitrosation [corrected]. Proc Natl Acad Sci U S A. 2004; 101:11471–11476. [PubMed: 15277664]
34. Samuel SM, Thirunavukkarasu M, Penumathsa SV, Koneru S, Zhan L, Maulik G, Sudhakaran PR, Maulik N. Thioredoxin-1 gene therapy enhances angiogenic signaling and reduces ventricular remodeling in infarcted myocardium of diabetic rats. Circulation. 2010; 121:1244–1255. [PubMed: 20194885]
35. Turoczi T, Chang VW, Engelman RM, Maulik N, Ho YS, Das DK. Thioredoxin redox signaling in the ischemic heart: an insight with transgenic mice overexpressing Trx1. J Mol Cell Cardiol. 2003; 35:695–704. [PubMed: 12788387]
36. Yamamoto M, Yang G, Hong C, Liu J, Holle E, Yu X, Wagner T, Vatner SF, Sadoshima J. Inhibition of endogenous thioredoxin in the heart increases oxidative stress and cardiac hypertrophy. J Clin Invest. 2003; 112:1395–1406. [PubMed: 14597765]
37. Ago T, Liu T, Zhai P, Chen W, Li H, Molkentin JD, Vatner SF, Sadoshima J. A redox-dependent pathway for regulating class II HDACs and cardiac hypertrophy. Cell. 2008; 133:978–993. [PubMed: 18555775]
38. Venardos K, Harrison G, Headrick J, Perkins A. Auranofin increases apoptosis and ischaemia-reperfusion injury in the rat isolated heart. Clin Exp Pharmacol Physiol. 2004; 31:289–294. [PubMed: 15191400]
39. Horstkotte J, Perisic T, Schneider M, Lange P, Schroeder M, Kiermayer C, Hinkel R, Ziegler T, Mandal PK, David R, Schulz S, Schmitt S, Widder J, Sinowatz F, Becker BF, Bauersachs J, Naebauer M, Franz WM, Jeremias I, Brielmeier M, Zischka H, Conrad M, Kupatt C. Mitochondrial thioredoxin reductase is essential for early postischemic myocardial protection. Circulation. 2011; 124:2892–2902. [PubMed: 22144571]
40. Chen X, Zhou HJ, Huang Q, Lu L, Min W. Novel action and mechanism of auranofin in inhibition of vascular endothelial growth factor receptor-3-dependent lymphangiogenesis. Anticancer Agents Med Chem. 2014; 14:946–954. [PubMed: 24913775]
41. Hom J, Sheu SS. Morphological dynamics of mitochondria--a special emphasis on cardiac muscle cells. J Mol Cell Cardiol. 2009; 46:811–820. [PubMed: 19281816]

42. Wencker D, Chandra M, Nguyen K, Miao W, Garantziotis S, Factor SM, Shirani J, Armstrong RC, Kitsis RN. A mechanistic role for cardiac myocyte apoptosis in heart failure. J Clin Invest. 2003; 111:1497–1504. [PubMed: 12750399]

43. Hayakawa Y, Chandra M, Miao W, Shirani J, Brown JH, Dorn GW 2nd, Armstrong RC, Kitsis RN. Inhibition of cardiac myocyte apoptosis improves cardiac function and abolishes mortality in the peripartum cardiomyopathy of Galpha(q) transgenic mice. Circulation. 2003; 108:3036–3041. [PubMed: 14638549]

44. Gerczuk PZ, Breckenridge DG, Liles JT, Budas GR, Shryock JC, Belardinelli L, Kloner RA, Dai W. An apoptosis signal-regulating kinase 1 inhibitor reduces cardiomyocyte apoptosis and infarct size in a rat ischemia-reperfusion model. J Cardiovasc Pharmacol. 2012; 60:276–282. [PubMed: 22635076]

45. Toldo S, Breckenridge DG, Mezzaroma E, Tassell BW, Shryock J, Kannan H, Phan D, Budas G, Farkas D, Lesnefsky E, Voelkel N, Abbate A. Inhibition of apoptosis signal-regulating kinase 1 reduces myocardial ischemia-reperfusion injury in the mouse. J Am Heart Assoc. 2012; 1:e002360. [PubMed: 23316291]

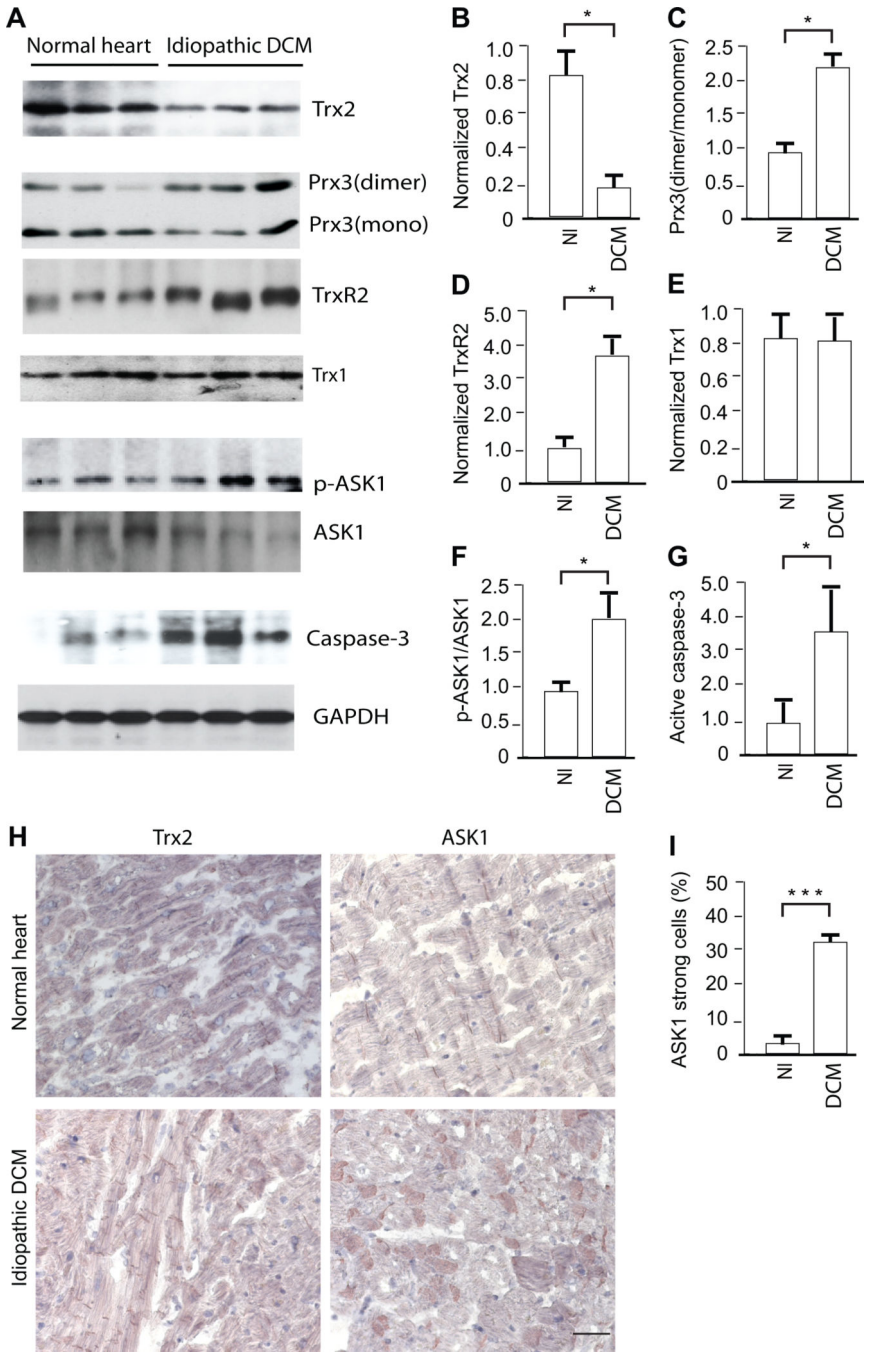

Figure 1.

Human hearts with cardiomyopathy show reduced Trx2 expression and increased ASK1 activity. Myocardial tissues were harvested from organ donors with preserved cardiac function (normal heart or Nl) and from cardiac transplant recipients with idiopathic dilated cardiomyopathy (DCM). **A**. Trx2, dimeric and monomeric Prx3, TrxR2, Trx1, phospho- and total ASK1, cleaved (active) Caspase-3 and GAPDH were measured by Western blot. Samples were from three individuals in each group. **B–G**. Normalized protein levels of Trx2, TrxR2, Trx1 and active Caspase-3 (to GAPDH) as well as the ratios of Prx3 dimer/

monomer and p-ASK1/ASK1 were quantified as fold of change in comparison to a value of the first normal heart sample arbitrarily set as 1.0. Data are presented mean±SEM, n=3, and analyzed by t-test using Prizm, **P*<0.05. **H–I**. Immunostaining for Trx2 and ASK1 in normal and diseased human heart, scale bar: 50 μm. ASK1 strong expressing cells are quantified (I). Data presented are mean±SEM, 3 fields per section and 5 sections from each myocardium. N=3, and analyzed by t-test using Prizm, ***, p<0.001. Considering the effects for factors “heart” and “field”, data were also analyzed using mixed effects model, p<0.001.

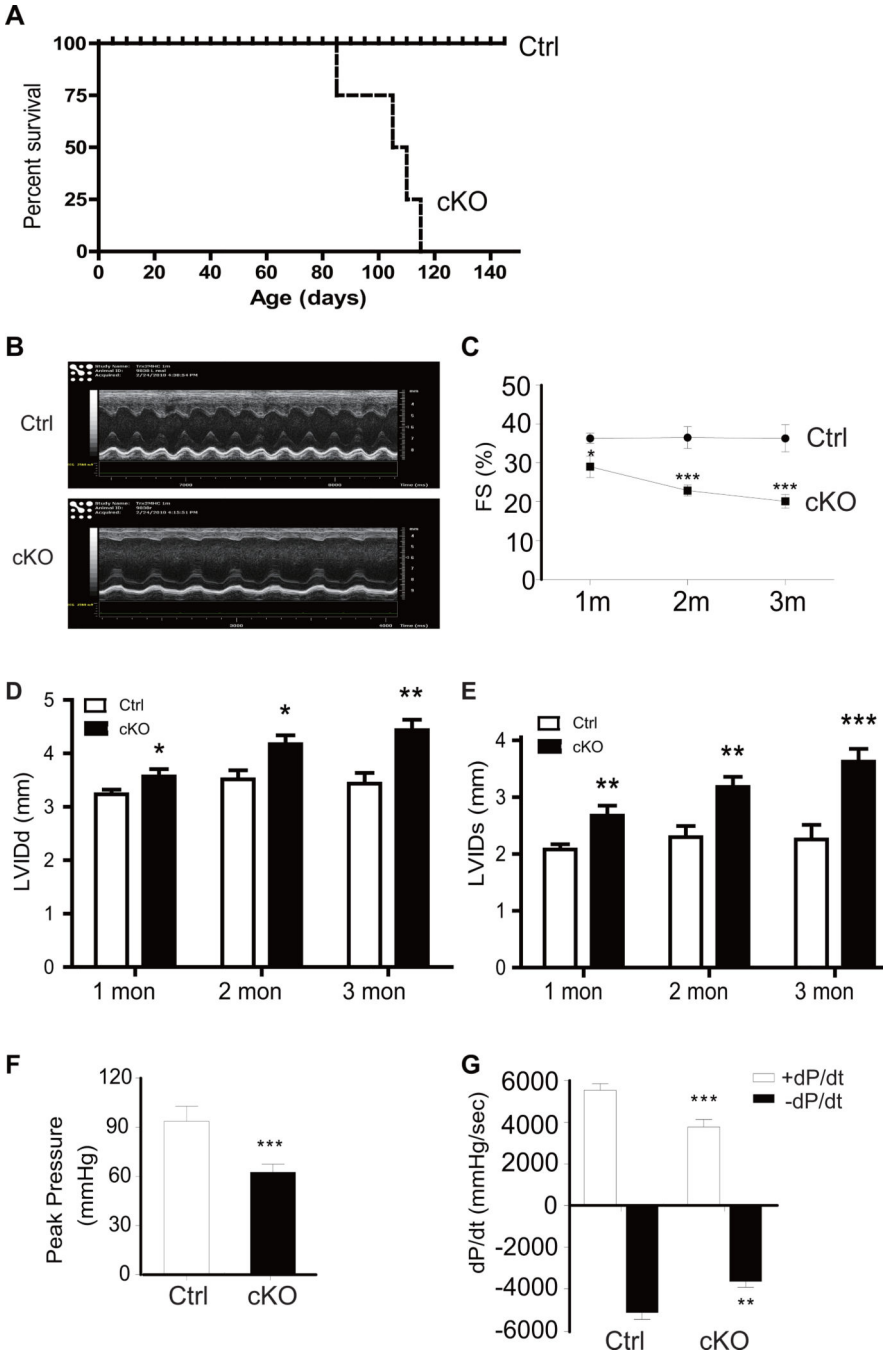

Figure 2.

Trx2-cKO mice exhibit dilated cardiomyopathy revealed by hemodynamic assessment. **A**. Cumulative survival curve of Trx2-cKO and Ctrl littermate mice. Trx2-cKO mice start dying from 90 days of age and 100% lethality was observed by 4 months of age (n=30 for Trx2-cKO and n=34 for Ctrl littermates). **B–E**. Echocardiographic analysis was performed in a separate cohort of animals at 1–3 month of age (n=10 per group in distinct subset of mice at each time point). Representative M-mode echocardiograms for 1 month old mice are shown in **B**. Trx2-cKO exhibited an age-dependent progression of cardiac dysfunction with

reduced fractional shortening (**C**), increased left ventricular internal dimension values at end-diastole (LVIDd) (**D**) and end-systole (LVIDs) (**E**). Data presented in C–E are mean ±SEM, n=10 mice per group, * $P<0.05$, ** $P<0.01$, *** $P<0.001$. **F–G**. Peak developed pressures and rates of pressure increase and pressure decrease during left ventricular contraction were measured by catheter in another cohort of 3 month old Trx2-cKO and Ctrl mice. The +dP/dt is the maximal rate of pressure development and −dP/dt is the maximal rate of decay of pressure. Data are mean±SEM, n=6, ** $P<0.01$, *** $P<0.001$.

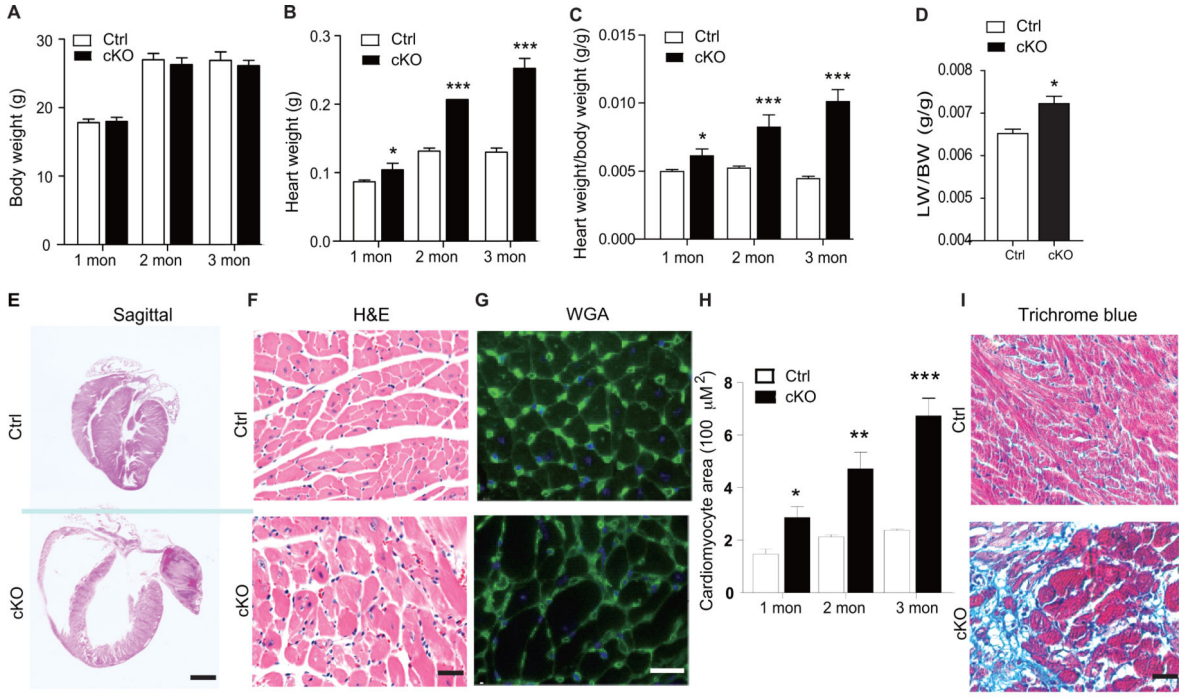

J

Wild Type	Trx2-cKO	Gene	Accession No.	Protein Name	Ratio
		Nppa	NM_008725.2	natriuretic peptide type A	17.3
		Nppb	NM_008726.4	natriuretic peptide type B	9.6
		Timp1	NM_011593.2	tissue inhibitor of metalloproteinase 1	6.9
		Acta1	NM_009606.2	actin, alpha 1, skeletal muscle	5.3
		Postn	NM_015784.2	periostin, osteoblast specific factor	5.2
		Myh7	NM_080728.2	myosin, heavy polypeptide 7, cardiac muscle, beta	4.4
		Tgfb2	NM_009367.1	transforming growth factor, beta 2	4.3
		Ctgf	NM_010217.2	connective tissue growth factor	3.5
		Serpine1	NM_008871.2	serine (or cysteine) peptidase inhibitor, clade E, member 1	3.4
		Lox	NM_010728.2	lysyl oxidase	2.8
		Fasl	NM_010177.3	Fas ligand	2.5
		Nox4	NM_015760.4	NADPH oxidase 4	2.5
		Rcan1	NM_001081549.1	regulator of calcineurin 1	2.1
		Acta2	NM_007392.2	actin, alpha 2, smooth muscle, aorta	2.1
		Sfrp1	NM_013834.2	secreted frizzled-related sequence protein 1	2.1
		Fhl1	NM_010211.2	four and a half LIM domains 1	2.0
		Prdx1	NM_011034.4	peroxiredoxin 1	-2.0
		Pdgfd	NM_027924.2	platelet-derived growth factor, D polypeptide	-2.0
		Ppp3ca	NM_008913.4	protein phosphatase 3, catalytic subunit, alpha isoform	-2.0
		Tnfrsf11b	NM_008764.3	tumor necrosis factor receptor superfamily, member 11b	-2.1
		Bnip3	NM_009760.4	BCL2/adenovirus E1B interacting protein 3	-2.2
		Esrra	NM_007953.2	estrogen related receptor, alpha	-2.2
		Tnnc1	NM_009393.2	troponin C, cardiac/slow skeletal	-2.2
		Gstp1	NM_013541.1	glutathione S-transferase, pi 1	-2.2
		Prdx3	NM_007452.2	peroxiredoxin 3	-2.3
		Ppp3cb	NM_008914.1	protein phosphatase 3, catalytic subunit, beta isoform	-2.4
		Nos3	NM_008713.4	nitric oxide synthase 3, endothelial cell	-2.4
		Cox4i1	NM_009941.2	cytochrome c oxidase subunit IV isoform 1	-2.4
		Map1lc3b	NM_026160.4	microtubule-associated protein 1 light chain 3 beta	-2.4
		Parp1	NM_007415.2	poly (ADP-ribose) polymerase family, member 1	-2.4
		Aifm1	NM_012019.2	apoptosis-inducing factor, mitochondrion-associated 1	-2.6
		Ppp3r1	NM_024459.2	protein phosphatase 3, regulatory subunit B, alpha isoform	-2.6
		Kcnd3	NM_019931.1	potassium voltage-gated channel, Shal-related family, member 3	-2.7
		Ndufa5	NM_026614.2	NADH dehydrogenase (ubiquinone) 1 alpha subcomplex, 5	-2.7
		Aldh2	NM_009656.3	aldehyde dehydrogenase 2, mitochondrial	-2.8
		Mmp9	NM_013599.2	matrix metallopeptidase 9	-2.8
		Hdac4	NM_207225.1	histone deacetylase 4	-2.9
		Tnnt2	NM_001130174.1	troponin T2, cardiac, transcript variant 1	-3.0
		Adrb1	NM_007419.2	adrenergic receptor, beta 1	-3.3
		Foxo3	NM_019740.2	forkhead box O3	-3.3
		Agtr1a	NM_177322.3	angiotensin II receptor, type 1a	-3.4
		Txn2	NM_019913.5	thioredoxin 2	-3.5
		Bcl2l11	NM_001284410.1	BCL2-like 11	-3.7
		Nampt	NM_021524.1	nicotinamide phosphoribosyltransferase	-4.0
		Myh6	NM_010856.2	myosin, heavy polypeptide 6, cardiac muscle, alpha	-4.0
		Ppargc1a	NM_008904.1	peroxisome proliferative activated receptor, gamma, coactivator 1 alpha,	-4.1
		Ppara	NM_011144.2	peroxisome proliferator activated receptor alpha	-4.2
		Tnni3	NM_009406.2	troponin I, cardiac	-4.4
		Ryr2	NM_023868.1	ryanodine receptor 2, cardiac	-4.6
		Hcn4	NM_001081192.1	hyperpolarization-activated, cyclic nucleotide-gated K+ 4	-5.0
		Sod2	NM_013671.3	superoxide dismutase 2, mitochondrial	-5.2
		Kcnd2	NM_019687.3	potassium voltage-gated channel, Shal-related family, member 2	-5.3
		Atp2a2	NM_001110140.3	ATPase, Ca++ transporting, cardiac muscle, slow twitch 2, transcript	-5.3
		Pln	NM_001141927.1	phospholamban, transcript variant 1	-6.2
		Adra1a	NM_013461.3	adrenergic receptor, alpha 1a	-11.4

Figure 3.

Trx2-cKO mice exhibit dilated cardiomyopathy revealed by structural and molecular analyses. **A–D**. Heart and lung tissues were harvested from Ctrl and Trx2-cKO mice at various ages. Body weight (A), heart weight (B), and heart weight /body weight ratios (C) were measured at 1–3 months of age. Lung weigh/body weight ratios (D) were quantified at 3 months of age. Data are mean±SEM, n=6, **P*<0.05, ***P*<0.01, ****P*<0.001. **E**. Biventricular enlargement of Trx2-cKO heart. Sagittal cross sections of hearts from Ctrl and Trx2-cKO mice were subjected to H&E staining. Representative heart images of 3-month

old Trx2-cKO *vs*. Ctrl littermates, scale bar: 1 mm. **F–H**. Cardiomyocyte size is increased in Trx2-cKO heart. Representative images of cross sections from 3-month old heart stained by H&E (F) and WGA immunofluorescence staining (G) are shown, scale bar: 50 μm. Cardiomyocyte cross-section areas at different ages were quantified in H. Data are mean ±SEM, averaged from 3 sections from each heart, n=6 mice per group at each age, **P*<0.05, ** *P*<0.01, ****P*<0.001. **I**. Trx2-cKO heart increases in fibrosis. Mason's Trichrome staining of ventricle sections from Ctrl and Trx2-cKO mice, scale bar: 50 μm, blue staining indicates fibrosis, n=6 mice per group. **J**. Gene expression analysis of myocardial tissue from WT and Trx2-cKO animals at 3 months of age was performed using Nanostring. Gene expression was normalized to the geometric mean of three housekeeping genes; ACTB, GAPDH and GTF2-β. Significant changes in gene expression between WT and Trx2-cKO that were 2-fold or greater were rank ordered and a heat map created using cluster analysis software (increase shown in red; decrease in green). Statistical analysis was performed using Student's 2-tailed *t* test, n=6 for each group, p<0.01 for all listed genes.

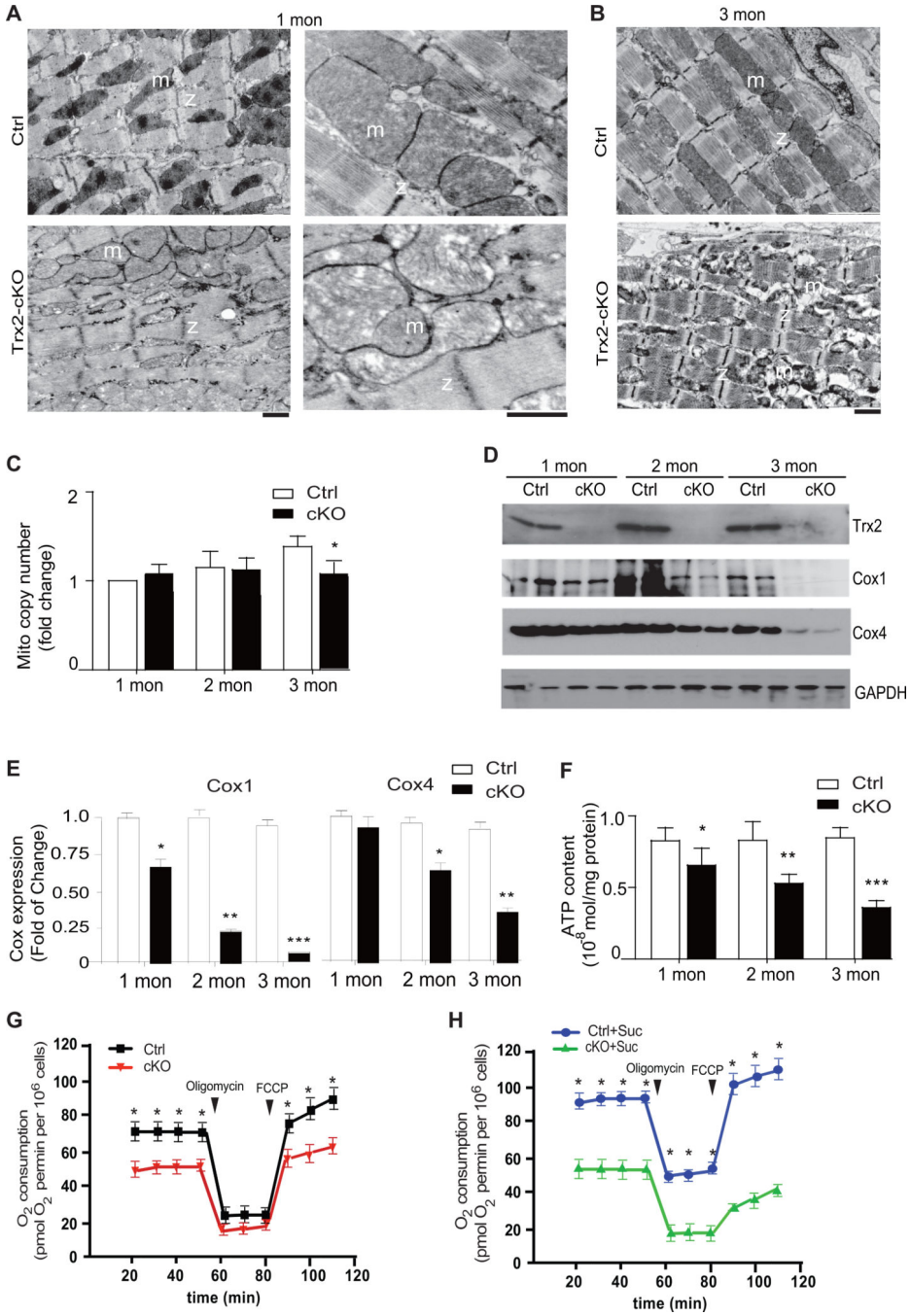

Figure 4.

Mitochondria in Trx2-cKO heart exhibit disrupted integrity and reduced function. **A–B**. Ultrastructural analysis of mitochondrial integrity by transmission electron microscopy. Representative electron micrographs of Ctrl and Trx2-cKO heart sections at 1 month (E, with higher magnifications on the right) and 3 months (F) of age. m: mitochondria; z: z-band, scale bar: 2 μm. **C**. Total DNA from heart tissues of Ctrl and Trx2-cKO mice were purified and subjected to quantitative PCR with specific primers for murine mitochondrial DNA and nuclear 18S rRNA gene. Mitochondrial DNA copies was normalized to 18S

rRNA and fold changes in Trx2-cKO heart tissue are presented by arbitrarily setting 1 month old Ctrl hearts as a value of 1.0. Data are mean±SEM, n=5 per group, **P*<0.05 vs. Ctrl littermates. **D–E**. Mitochondrial cytochrome c oxidase (COX1 and COX4) expression in Ctrl and Trx2-cKO heart tissues were determined by immunoblotting at 3 day to 3 months of age. The levels of COX1 and COX4 were not significantly altered on day 3 (not shown). Fold changes in protein expression were normalized by arbitrarily setting 3-day heart sample values as 1.0. n=4 at each time point, **P*<0.05, ***P*<0.01, ****P*<0.001. **F**. Adenosine triphosphate (ATP) content, an indicator of mitochondrial function, was measured in Ctrl and Trx2-cKO heart tissues and expressed as mol/mg protein. Data are means±SEM, n=6, ***P*<0.01, ****P*<0.001. **G–H**. Oxygen consumption rate in cardiomyocytes isolated from Ctrl and Trx2-cKO heart under basal conditions, following the addition of the ATP coupler Oligomycin (1 μM), and then the electron transport chain accelerator carbonyl cyanide-p-trifluoromethoxyphenoylhydrazone (FCCP; 1 μM) using assay buffer (G) or in the presence of succinate (5 mM) (H). Data are mean±SEM from three independent experiments, and analyzed by repeated measure two-way ANOVA, *, *P*<0.05.

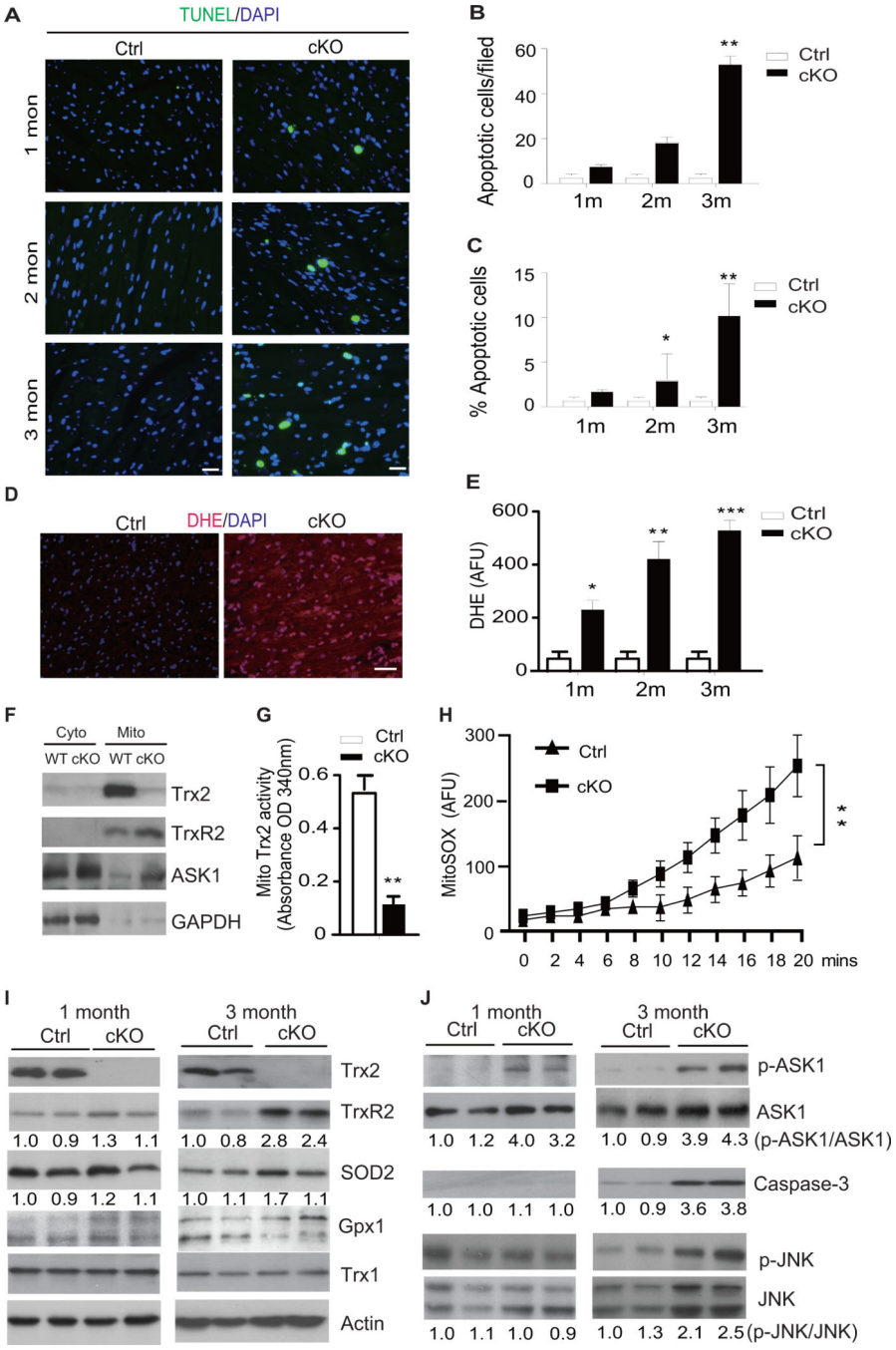

Figure 5.

Cardiac-specific Trx2 deletion induces mitochondrial ROS production and ASK1 activation with enhanced cellular apoptosis. **A–C**. TUNEL staining of heart tissue sections from Ctrl and Trx2-cKO mice at 1–3 months of age. Representative images are shown in A, scale bar: 50 μm. TUNEL-positive cells per 200× field (top) and the % of apoptotic cells (bottom) were quantified in B–C. Data are mean±SEM, n=3 mice for each time point, results averaged from 3 sections from each heart, * $P<0.05$, ** $P<0.01$, and *** $P<0.001$. **D–E**. Fresh heart tissue from Ctrl and Trx2-cKO mice at 1–3 months of age were stained with

DHE. Representative images are shown in D, scale bar: 50 μm. DHE fluorescence intensity per 200× field were quantified in E. Data are mean±SEM from three independent experiments averaged from 10 randomly selected fields for each sample, ***P*<0.01, ****P*<0.001. **F–H**. Effects of Trx2 deletion on mitochondrial ROS. Cytosolic and mitochondrial fractions were isolated from 1 month old Ctrl and Trx2-cKO hearts. Expression of Trx2, TrxR2, ASK1 proteins and GAPDH were determined by immunoblotting (F). Trx2 activity was measured using an insulin disulfide reduction assay in mitochondria-enriched fractions (G). ROS production from intact mitochondria was measured by MitoSOX probe in a fluorescence plate reader for 20 min (H). Data presented in G and H are mean±SEM, n=6 mice in each group, ***P*<0.01. **I–J**. Effects of Trx2 deletion on the expression of sevral cellular anti-oxidants (I) and ASK1 signaling proteins (J) were determined by immunoblotting. Two heart tissue samples from each group at ages of 1 and 3 months of age are shown. Similar results were obtained from two additional experiments.

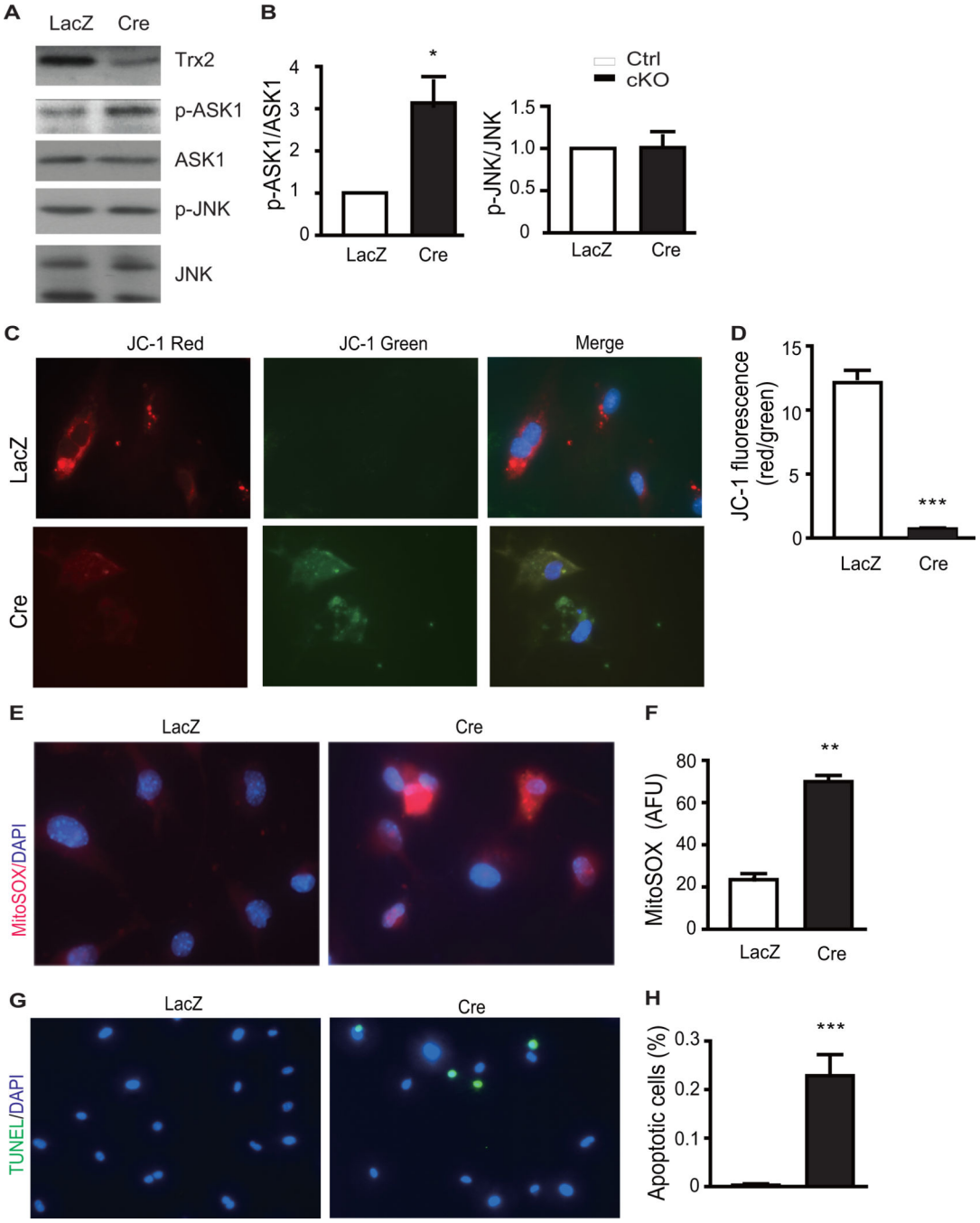

Figure 6.

Deletion of Trx2 in cardiomyocytes induces mitochondrial dysfunction with increased cellular ROS and apoptosis. Neonatal cardiomyocytes isolated from $Trx2^{lox/lox}$ mice were infected with adenovirus expressing LacZ or Cre recombinase (to induce Trx2 gene deletion). At 48 h post-infection, the cells were subjected to ASK1 activity, mitochondrial function, ROS and apoptosis analyses by immunofluorescence microscopy. **A–B**. Effects of Trx2 deletion on ASK1 signaling were determined by immunoblotting. Similar results were obtained from two additional experiments. Ratios of p-ASK1/ASK1 and p-JNK/JNK were

quantified in D as fold change by normalizing to LacZ (arbitrarily set as 1.0). Data are mean ±SEM, n=3. **P*<0.05. **C–D**. Mitochondrial membrane potential (ΔΨm) measurement with the JC-1 probe. Representative red and green images from three independent experiments are shown. Densitometric analysis of JC-1 fluorescence intensities, decreased red/green ratio indicates decreased mitochondrial membrane potential. **E–F**. Generation of ROS in Ctrl and Trx2-cKO neonatal cardiomyocytes was evaluated with MitoSOX staining. Quantification of MitoSOX fluorescence intensities as arbitrary fluorescence units (AFU). **G–H**. Isolated neonatal myocytes were stained for apoptosis by TUNEL assay. Quantification of TUNEL assay: apoptotic nuclei were scored on the basis of TUNEL positive cells. Data in D, F and H are mean±SEM from three experiments in 10 randomly selected fields from each group, ****P*<0.001 vs. control.

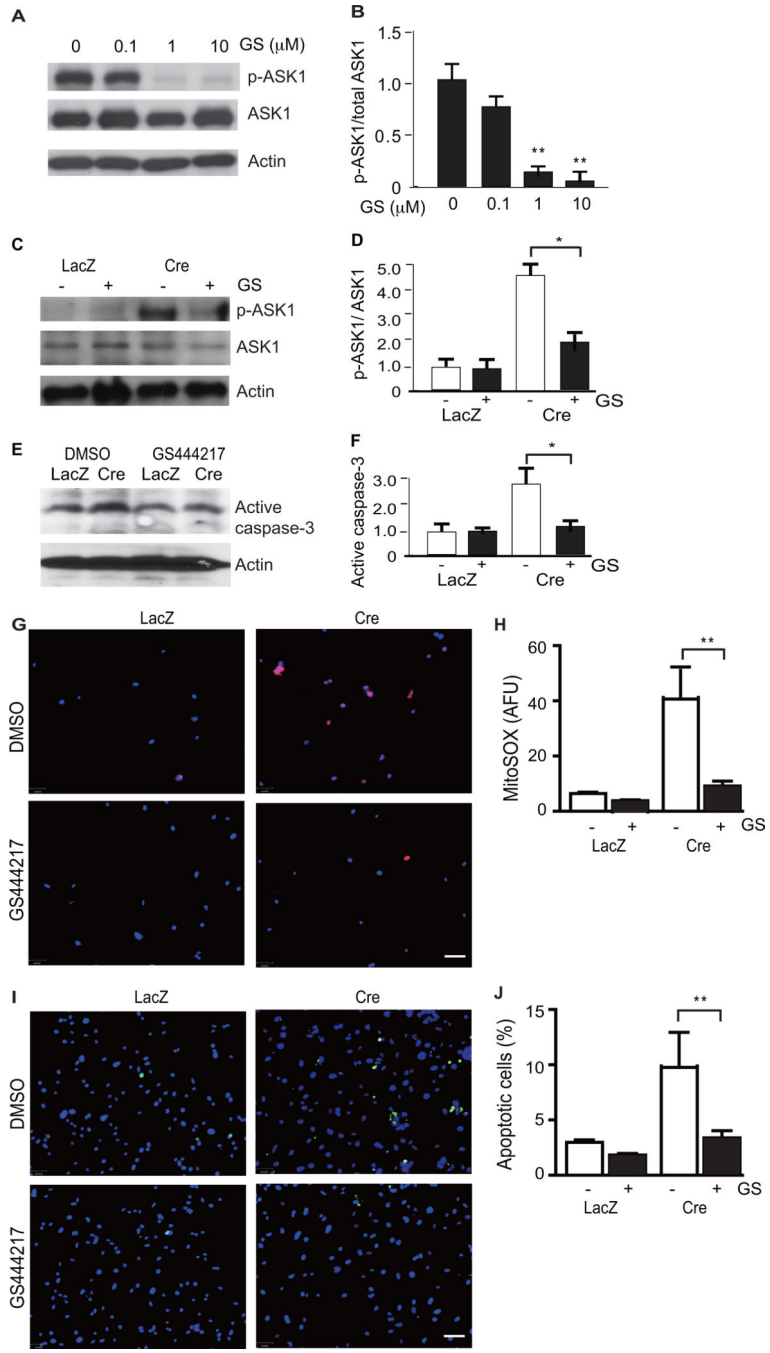

Figure 7.

ASK1-specific inhibitor blocks Trx2 deletion-induced ASK1 activation, mitochondrial dysfunction, ROS and cellular apoptosis. **A–B**. ASK1i dose response. GS-444217 at 1 μM strongly inhibits ASK1 overexpression-induced autophosphorylation at pT845. An ASK1 expression plasmid was transfected into 293T. At 24 h post-transfection, cells were treated with GS-444217 at 0, 0.1, 1 μM or 10 μM for 6 h. Phosphorylations of ASK1 was determined by Western blotting. Total proteins of ASK1 and β-actin were also determined. Ratio of p-ASK1/ASK1 was quantified as fold changes by normalizing to untreated control

(arbitrarily set as 1.0). Data are mean±SEM, n=4, ***P*<0.01. **C–J**. ASK1i on Trx2 deletion-induced responses. Neonatal cardiomyocytes isolated from $Trx2^{lox/lox}$ mice were infected with adenovirus expressing LacZ or Cre recombinase and the cells were cultured in the presence or absence of an ASK1 inhibitor, GS-444217 (1 μM) for 48 h. Effects of Trx2 deletion on ASK1 signaling (C–D) and Caspase-3 activation (E–F) were determined by immunoblotting with phosphor-ASK1, total ASK1 and cleaved Caspase-3-specific antibodies. Similar results were obtained from two additional experiments. Ratios of p-ASK1/ASK1 (D) and active caspase-3 (F) were quantified as fold change by normalizing to LacZ (arbitrarily set as 1.0). Data are mean±SEM, n=4. **P*<0.05. G–H. ROS analyses were performed by immunofluorescence microscopy using the mitochondria-specific ROS probe MitoSOX. I–J Apoptosis analyses were performed by immunofluorescence microscopy by TUNEL staining. Representative images from three independent experiments are shown in G and I. Quantification of ROS and apoptosis are shown in H and J. Data are mean±SEM from three experiments, ***P*<0.01.

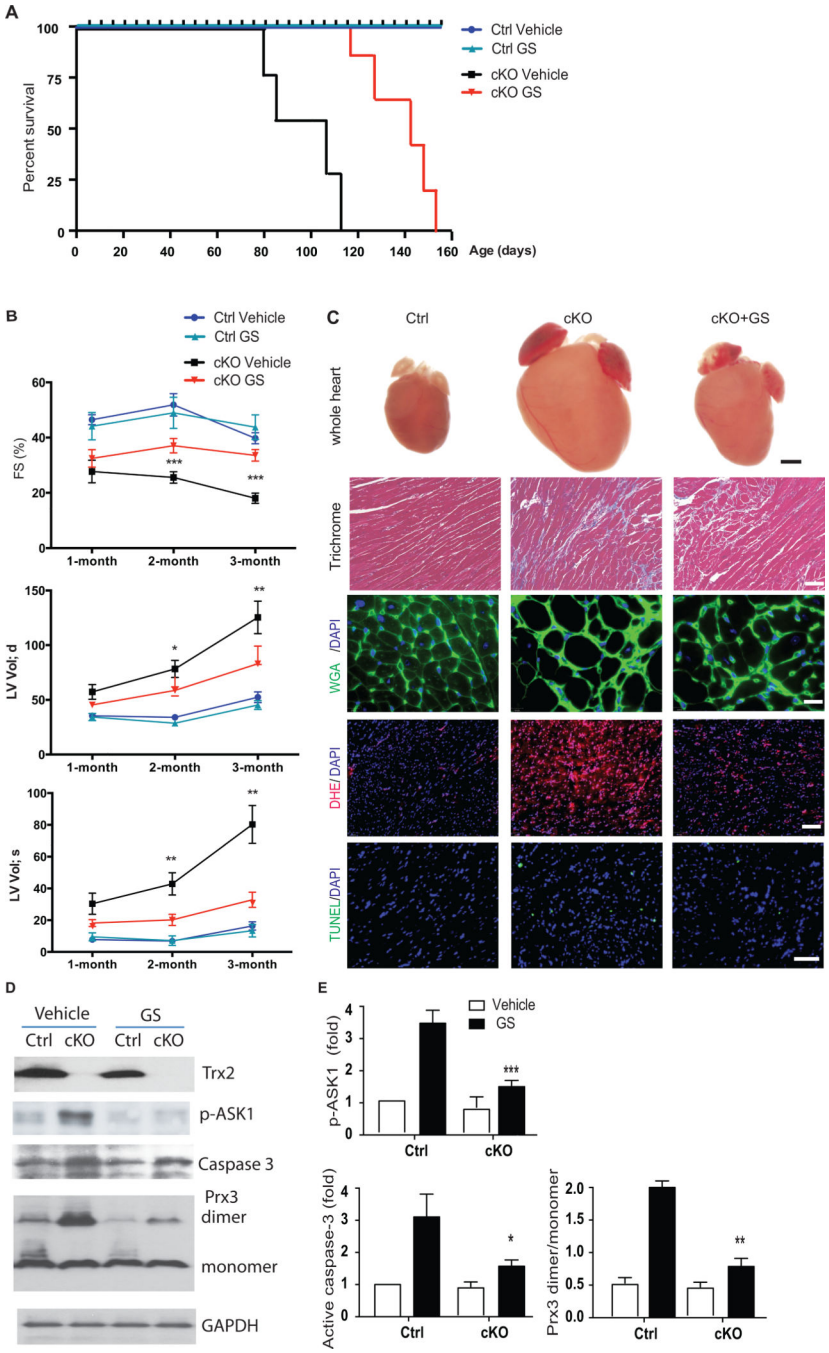

Figure 8.

ASK1-specific inhibitor reduces cardiac dysfunction and cardiomyopathy phenotype in Trx2-cKO mice. Ctrl and Trx2-cKO mice were mouth-fed with vehicle or the ASK1-specific inhibitor GS-444217 in solution once a day from P10 to P27. Mice were weaned at P27 and fed a chow diet with or without GS-444217 for 3 months. **A**. Effects of ASK1i on the cumulative survival curve of Trx2-cKO and Ctrl littermates. All GS-treated Trx2-cKO mice survived beyond 115 days of age when 100% lethality for untreated Trx2-cKO mice was observed, n=15 in each group, $P<0.001$ Trx2-cKO/GS vs. Trx2-cKO/vehicle. **B**. Effects

of ASK1i on cardiac function of Trx2-cKO at 1–3 month ages by echocardiographic analysis of a single cohort of animals. ASK1i reduces age-dependent progression of cardiac dysfunction with reduced fractional shortening (%FS), increased left ventricular volume at end-diastoles and end-systoles (LV VOLd and LV VOLs). Data are mean±SEM, n=10 mice per group, analyzed by repeated measure two-way ANOVA, ***, $P<0.001$ Trx2-cKO/GS *vs*. Trx2-cKO/Vehicle. **C**. Histology, ROS, and apoptosis were measured at 3 months of age. Whole hearts (scale bar: 1 mm) show that GS-444217 decreases four-chamber enlargement in Trx2-cKO mice. Trichrome blue, WGA, DHE and TUNEL staining were performed to assess fibrosis, cardiomyocyte hypertrophy, ROS production and apoptosis, respectively. Representative images from Ctrl/Vehicle, Trx2-cKO/Vehicle, and Trx2-cKO/GS are shown, scale bar: 50 μm. **D–E**. Effects of ASK1i on ASK1 signaling at 3 months of age. Phosphorylation of ASK1, active caspase-3, Prx3 monomers and dimers were determined by immunoblotting. Representative images from n=5 are shown in D. Normalized Trx2 expression, phosphorylation of ASK1, active caspase-3 and the ratios of Prx3 dimer/monomer were quantified in E as fold change in comparison to vehicle-treated Ctrl mice (arbitrarily set as 1.0). Data are mean±SEM, n=5, * $P<0.05$, ** $P<0.01$, ***<0.001 Trx2-cKO/GS vs. Trx2-cKO/Vehicle.